

Response to reviewers' comments of Olin et al.: "CFD modeling of a vehicle exhaust laboratory sampling system: Sulfur driven nucleation and growth in diluting diesel exhaust"

We thank the reviewers for their detailed and very useful comments, and have corrected the manuscript according to them.

Referee reports are in *black italic* and authors' response is in **blue roman** font. The changes to the manuscript are provided as the marked-up manuscript at the end of this file.

Referee 1 report and authors' comments:

Olin et al. study nucleation in diesel exhaust using CFD tools. It's a nice piece of work but the presentation could be significantly better. Findings should be discussed more in-depths, underlying reasoning explained, most of the figures need to be re-done since they are so tiny, and the manuscript's English needs some serious work. In the following, I will give detailed comments on contents and presentation issues BUT I feel that bringing the language up to par is far beyond any reasonable review demand.

Most of the figures are improved; they are clearer now. A language check is also done throughout the manuscript.

p. 2908, l. 23f "Two versions of the model code, an Eulerian and a Lagrangian model, are presented."

Why two models? What's the motivation?

While the Eulerian model can provide the spatial information inside the sampling system, the Lagrangian model cannot. However, the Eulerian model can suffer from poorer spatial resolution that is caused by the higher amount of dimensions to be simulated compared to the Lagrangian model, if the same computational costs for the both models are considered. A poor spatial resolution can cause unrealistic results because of the discretization of the transport equations inside the computational cells. Comparing the results obtained from the both models provides information on the sufficiency of the spatial resolution of the Eulerian simulation. The corresponding text in the manuscript is clarified.

p. 2910, l. 23f "A steady-state simulation is performed, where all time derivatives are zero, which provides shorter computation time."

I don't think it's necessary to define what steady-state means. I would expect readers to know. Instead it would be nice to have a sentence like "the nature of the setup (no time-dependence) allows for a steady-state approach which saves time" that motivates why steady-state is possible and desirable.

The text is changed towards your suggestion.

p. 2911, l. 8f “but the influence of nucleation and condensation on the properties on the fluid side is negligible.”

Is it? Has it been tested? How large is the effect? With sulfuric acid between 10^{-9} and 10^{-11} and $J 10^{-7}$ it doesn't seem all that clear-cut even if the residence time is very short. Given that you have the other model that includes feedback it would be quite easy to qualify and quantify this statement. Readers cannot be expected to take it on faith, can they?

Sulfuric acid, water, and hydrocarbon vapors decrease only about 4%, 1%, and 1%, respectively, during the whole simulation domain of the Eulerian simulation in A cases. Therefore, gas-to-particle conversion and the particle loading have only little effects on the fluid side composition, and one-way coupling can be considered a sufficient approximation. The corresponding text in the manuscript is improved.

p. 2911, l. 16ff “Due to fewer dimensions in Lagrangian model compared to the Eulerian model, a very high temporal resolution can be simulated. That can be used to ensure the sufficiency of spatial resolution of the computational grid of the Eulerian model by comparing the results from both models.”

Well, how exactly? When the high-res model uses input from the low-res model, how does it work as quality control?

The Lagrangian model uses low-res inputs from the Eulerian model for temperature and gas species concentrations, but particle dynamics computation is done in high-res in the Lagrangian model. Therefore, the quality control is done by comparing the particle distribution results between the low-res and the high-res particle dynamics computation. The corresponding text in the manuscript is clarified.

p. 2911, l. 24f ““Nucleation” is a key process controlling particle number concentration in diluting exhaust is particle formation, which is generally considered sulfur-driven.”

Too many verbs in the first part of this sentence. Please re-write. I would also take issue with the word sulfur-driven. It's really sulfuric acid, isn't it?

There was one “is” word too much; it is now removed from the manuscript. The most of the studies done for diesel exhaust nucleation connect the particle concentration to the fuel or oil sulfur due to the lack of the sulfuric acid measurement; therefore, a typical conclusion is that nucleation is considered sulfur-driven instead of sulfuric acid-driven. However, sulfuric acid is now mentioned too in the sentence of the manuscript.

p. 2912, l. 10f “Nucleation exponents 1 and 2 are found to fit to atmospheric measurement results better than the values from CNT (Sihto et al., 2009),”

*That may be true in Finland, but not, for example, in China. Never mind if CNT works there, but values well above 2 have been observed. www.atmos-chem-phys.net/11/12663/2011/
www.atmos-chem-phys.net/14/2169/2014/*

The references are now added to the manuscript.

p. 2912, l. 28f “until recently”

One could argue that this is a rather liberal use of the word “recently”. Various instruments and techniques to go below 3nm have been around for quite some years already. In fact, given the size ranges in the manuscript, a PSM could really provide some valuable additional insight.

The sentence is now changed in the manuscript, and the reference to PSM is added.

p. 2913, l. 3ff “Particle dynamics, such as condensation and coagulation, alter the particle distribution during the time, when newly formed clusters grow to measurable sizes. Therefore, the actual and the observed nucleation rates are unequal and their nucleation exponents can be different too.”

This is rather trivial, so why write it? There seems to be something missing to make this an actual thought.

There was actually nothing missing, it was just a trivial thing. The sentences are now shortened.

p. 2914, l. 2 “in this case”

Do you mean “in this study”?

Yes. It is corrected now.

p. 2914, l. 2f “In this case, the following nucleation scheme is used:”

Why this scheme and not some other? I mean, there is plenty to choose from. It would be nice to hear reasons as surely there must be some.

The scheme is chosen because it is the simplest form of a nucleation scheme where the dependencies of sulfuric acid and water vapors and temperature are included. Saturation vapor pressure of sulfuric acid is included because of its exponential temperature-dependency, which is also the case of nucleation rate. The corresponding text in the manuscript is now improved.

p. 2917, l. 8f “slightly higher sulfuric acid concentrations”

What does slightly mean here? Fuel sulfur content is 6-fold, to what difference in sulfuric acid concentrations does that translate?

50 % in maximum sulfuric acid cases. That is now added to the sentence.

p. 2917, l. 10ff “Volatile nucleation mode concentration increased in both measurements, when sulfuric acid concentration increased over the time, though all the operation parameters remained constant.”

What exactly is the point of this sentence? In itself it seems rather trivial: more sulfuric acid leads to more nucleation. Is this supposed to me a summary of the experiments? If so, something more and less obvious could be nice.

There were information missing on that sulfuric acid concentration and volatile nucleation mode concentration increased slowly, though the operation parameters remained constant in the experiments. That is due to the unsteadiness of the storage effect of the after-treatment system. This is now added to the manuscript.

p. 2917, l. 14ff

The whole paragraph is written in a funny way. First you say what the domain consists of. Then you go on describing some part that is not included without stating explicitly that this part has been left out. This could be re-written to be clearer. The corresponding picture needs a serious makeover. There should really be two figures, one with the experimental setup, and one just showing the computational domain. And the figure needs to be way clearer. Thin lines, tiny letters, it’s really not a pleasure to look at. You might also want to reconsider if making it to scale is such a great idea. I would prefer clarity.

The text in the paragraph is clarified. Additional figure showing the experimental setup is added. The figure of computational domain is re-drawn to be clearer.

p. 2917, l. 27 “gaseous sulfuric acid”

Say vapor instead. Sulfuric acid vapor. It is a gas, yes, but in the context of this work it is much clearer to use gas for air and vapor for the stuff that condenses (water, sulfuric acid, . . .). I would change this throughout the text. Generally, in aerosol physics, one speaks of condensable vapors. It’s merely a convention but it is useful to distinguish what role a compound plays in a system (carrier gas, condensable vapor, or whatever). It makes everything much clearer.

It is now changed throughout the text. “Gaseous sulfuric acid” is commonly used in exhaust measurement publications.

p. 2918, l. 12 “lambda value”

Would be nice to have a definition here.

“the fraction of injected air mass compared to the air mass required for the stoichiometric combustion“ is now added to the text.

p. 2918, l. 13f “RH was not measured, but RH = 10% can be considered an upper limit”

And the reason for this is?

10% is the upper limit, because the pressure of the compressed air used for the dilution air was 10 bar. This is now added to the text.

p. 2918, l. 14f “Total hydrocarbon mole fraction (except for volatile hydrocarbons) was fitted to obtain the measured volatile nucleation mode particle sizes.”

This needs some explanation. What was fitted to what and why?

The text is now changed to a clearer form: “Total hydrocarbon mole fractions (except the most volatile hydrocarbons) in the raw exhaust were set to the values that produce the measured volatile nucleation mode particle sizes (the diameter of a particle with the average volume) at the outlet.”

p. 2918, l. 21 “but the cooling is not simulated here”

Why not? Given that it actually makes a difference. . .

The cooling effect of the dilution air is not simulated, because it would require the modeling of the dilution air before the dilution air inlet boundary. That would be more challenging simulation due to the porousness of the diluter and due to the requirement for a 3-D simulation. The corresponding text in the manuscript is now improved.

p. 2919, l. 8 “onto which liquids condense and coagulate”

This sounds a bit funny. I thought vapors condense and particles coagulate.

The text is now changed to “onto which vapors could condense and which are coagulated with volatile nucleation mode particles”.

p. 2919, l. 11f “the assumption that soot particles do not grow by condensation but gases condense into empty spaces of the fractal particles”

That would imply that residence times are too short for condensation to fill all the gaps and the particle to grow beyond its initial size. Is that so?

All the gaps will actually be filled in some cases, but the particle growth beyond their initial sizes are still not very significant. The following text about the validation test is now added to the manuscript: “The validity of the assumption was tested by calculating the mobility diameter in the case where condensation is most dominant; if all the empty spaces of the fractal particles were filled with the condensing vapors and the coagulation from the volatile nucleation mode were taken into account, CMD would increase to the value of about 60 nm in maximum. Therefore, the assumption CMD remains as the value of 49 nm could be a valid approximation.”

p. 2920, l. 22 “relevant size of a particle from which atmospheric aerosol formation starts”

Can this atmospherically relevant size simply be transferred to the largely different conditions (temperature, vapor concentrations etc) in diesel exhaust?

No, it is not that simple. The following text is now added to the manuscript: “However, the atmospherically relevant size may not be simply transferred to the clearly different conditions (such as temperature and vapor concentrations) prevailing in vehicle exhaust, but it is used here due to a lack of detailed information on that.”

p. 2921, l. 7f “Figures 4 and 5 show that nucleation begins at the boundary of hot exhaust and cold dilution air.”

Well, actually, those figures show very little because they are very, very small. The same applies to the following figures. Also, we don’t really see that nucleation begins at the boundary of hot and cold air. There is no temperature information in the figure, so how could we possibly see that? In general, these nice, colorful figures show very little detail. I would like to see some T and J profiles along the radius to actually be able to observe the difference between the nucleation exponents.

The contour plot figures are scaled vertically. An additional contour plot about temperature field is added. T and J profiles along the axis are also added where the difference between the nucleation exponents is seen clearer. The profiles along the radius do not show the difference as clear as along the axis.

p. 2921, l. 16f “In R cases, volatile nucleation mode number concentration was decreased 3–9% due to coagulation, depending on the case. Cases with smallest particles had the highest coagulation losses due to increased coagulation coefficient. Coagulation to soot mode contributed over 70% of the total coagulation loss.”

Is the assumption that soot doesn’t grow still used here? Is it justified with all that coagulation going on?

The assumption is still used here. The validity test was included to the same that is mentioned before in the case of condensation to the empty spaces of the fractal particles.

p. 2922, l. 6ff “CMDvol at the outlet in R cases was obtained by fitting simulated and measured diameters of average volume with the amount of hydrocarbons in raw exhaust.”

This could be clearer. What was fitted to what and which parameter was adjusted?

This was actually a repetition of the unclear fitting sentence mentioned before. This sentence is now removed from the manuscript.

p. 2922, l. 16ff “However, CMDvol would increase then, but not with as fast growth rate as CMDcore, due to smaller particle size.”

Really? In atmospheric observations, the growth rate often decreases with particle size which is intuitively quite simple: in the case of bigger particles, the same growth rate requires much more condensable vapor. What’s working against that in this case? Kelvin? Collision rate?

There were several errors in the whole paragraph that made the message unclear. The growth rate of course decreases with increasing particle size, which was actually the point of the text. The text of the paragraph is now improved in the manuscript.

p. 2924, l. 6ff “The time domain was divided to 10^6 time steps, which corresponds to a higher resolution compared to the Eulerian simulation, where the paths pass through 6000–8000 computational cells.”

What exactly is the benefit of this? If I understood correctly, the model is fed with output from the CFD domain which has much poorer resolution.

The resolution is different for the gas concentration and for the particle dynamics as mentioned before in this file.

p. 2924, l. 23f “However, the difference of the concentrations can also be partially accounted for numerical error caused by the lower resolution in the Eulerian simulation.”

This of course needs some explanation. By what mechanism is the difference produced?

The lower resolution can produce higher concentrations if nucleation rate is high in some computational cells, and where nucleation rate remains constant in the cell (intracellular changes of the vapor concentrations are not included), and too high particle number is formed. However, the effect of the diffusive particle transfer from the higher particle concentration is found to be the main effect in this case; therefore, the unclear sentence is now removed from the manuscript. A new figure with particle concentration without turbulent diffusion is now added, which clarifies the effect of the diffusion flux to the path lines.

p. 2925, l. 1 “some numerical error exists”

That sounds like a euphemism. It seems like a bit of a mess. Can you explain what exactly is happening there? “Numerical error” is rather vague.

A better explanation for the “numerical error” for J, N, CMD, and GSD is found in more detailed examination of the flow field. The “error” is actually the fluctuation of variables caused by turbulent eddies formed at the end of the porous section. A new figure with CMD without turbulent diffusion is now added, which clarifies the effect of the diffusion flux to the path lines.

p. 2925, l. 13 “It can be executed with very high time resolution”

Again: what is the point of high time resolution if the input data doesn't have the same resolution?

The resolution is different for the gas concentration and for the particle dynamics as mentioned before in this file.

p. 2925, l. 21 “too low”

Too low for what?

The sentence is now changed to “the spatial resolution may remain too low to be able to produce realistic results, if the same computational effort as for the Lagrangian model is considered.”

p. 2926, l. 4f “which is the cut-size D50 of used particle counter TSI CPC 3025”

Well, cut sizes differ from unit to unit, even if it's the same model. One also has to keep in mind that the detection efficiency curve is not a step function. So while this is the best thing that can be done in this situation, it is not more than a rough estimation.

“Particles larger than D_{50} ” is replaced by the detection efficiency curve. That has only a small effect on the figure and do not change the conclusions. The corresponding text is also changed so that the reader understands that the detection efficiency curve is not defined for the exactly same unit as used in the exhaust measurements.

p. 2953, figure 10

It would be MUCH better to include those lines in one of the improved figures 4-8. That would provide some context. In any case, the figure in its current form is not very enlightening and needs some thinking about.

The path lines are now included in the new temperature contour figure.

p. 2954, figure 11

Where does all the noise between 0.02 and 0.03 come from? Also those jumps for the right curves seem somewhat unphysical. What's happening there?

The noise are caused by the fluctuation of variables caused by turbulent eddies formed at the end of the porous section. There were no unphysical jumps in the curves; the time scales for the left and for the right plots were different. The corresponding text is now clarified in the manuscript, and the figure is re-drawn in a clearer form. The number of path lines is also decreased from 3 to 2 to keep the figures clear.

p. 2955, figure 12

With all the noise it's kinda hard to determine what the actual message of the figure is. I can't offer any good ideas but it would be nice to present this in a clearer way.

This figure is also re-drawn now.

Referee 2 report and authors' comments:

Report in the technical review phase (page and line numbers do not correspond to the published discussion article, and the marked-up manuscript does not show the changes made during the technical review phase):

The study of Olin et al. deals with CFD modeling of the aerosol processes during sampling of diesel exhaust under specific laboratory conditions. The focus is on nucleation process although the significance of other processes (condensation, coagulation, diffusion and deposition) is studied as well. The applied model is an extension of an older model developed in their laboratory and built around the modal representation of the aerosol size distribution. Their aim is to evaluate the applicability of the model to study particle formation involving sulfuric acid in diesel exhaust using previously published data. They used two types of sub-models (Eulerian and Lagrangian) and found that both models produced almost the same results and hence their model can be used to examine particle formation with lower computational cost compared to sectional models. As regards particle formation, they found that although the highest nucleation rates exist at the interface of hot exhaust and cold dilution air, the nucleation remains high during the aging of the mixture resulting to the formation of 99% of the nucleation particles in the aging chamber. Furthermore, they found that the major part of deposition occurs in the expander of the aging chamber but its influence was significant for solid particles only, since most of volatile nucleation mode particles were formed later during the aging process. The most critical point of the work was the values of nucleation exponents which were different for the two cases of experiments tested (see below in specific remarks).

The paper is well written and easy to follow (although some improvements are necessary). The title is good, containing the necessary information and the abstract reflects the points made in the paper. The introduction is adequate in general but it would be better if some more appropriate information concerning the rationale of the work was given (see below). The procedure followed is based on the current knowledge gained from atmospheric research, that is, analysis of correlations between measured concentrations of newly formed particles and sulfuric acid concentrations, extended to include variation of temperature and relative humidity. The analysis of the results is comprehensive and the data presented seem adequate to support the conclusions providing new, relevant insights. The literature is good in general (see below for some papers that could be added in the discussion) and figures and tables are clear enough.

In conclusion, the paper is very interesting and merits publication. It shows how specific laboratory measurements can be used to determine the mechanism responsible for nucleation events during exhaust sampling. I think, however, that the picture would be better if the authors address the comment given below.

Specific comments

*The Introduction starts with reference to ultrafine particles and their significance from a health perspective. Although this start is classical in recent aerosol papers, I think that the main issue in this work is nucleation mode particles found in the diesel exhaust and hence the introduction would be better if the authors referred to the health importance of these particles. I think that the paper of Alföldy et al., 2009 “Size-distribution dependent lung deposition of diesel exhaust particles”, *Aerosol Science* 40 (2009), pp. 652 – 663 is more relevant and should be added as well as that of Rissler et al., “Experimental determination of deposition of diesel exhaust particles in the human respiratory tract”, *Journal of Aerosol Science* 48, 18–33. Another useful paper not mentioned is that of Mathis et al., 2004 “Effect of organic compounds on nanoparticle formation in diluted diesel exhaust” *Atmos. Chem. Phys.*, 4, pp. 609–620. I think that this work should absolutely be referenced in the paper; not to say to be discussed, since it is relevant with one of the authors’ assumptions concerning nucleation (organics).*

These three references are worth of mentioning in this paper.

The first paragraph in Introduction is changed to:

“Ultrafine particles are related to adverse health effects (Dockery et al., 1993; Pope et al., 2002; Beelen et al., 2014) and various effects on climate (Arneth et al., 2009). Diesel vehicles have a significant role on the health effects, because they have a major contribution to ultrafine particles of urban air (Virtanen et al., 2006; Johansson et al., 2007; Pey et al., 2009) and because the sizes of the particles emitted by diesel vehicles lie in the range of high lung deposition probability (Alföldy et al., 2009; Rissler et al., 2012).”

which now includes the references Alföldy et al. 2009 and Rissler et al. 2012.

In page 8, line 15, the following sentence is added:

“Mathis et al. (2004a) have experimentally determined that some organic compounds are capable of initiating and increasing or decreasing (depending on the functional groups) nucleation mode particles emitted by a diesel engine.”

which includes the reference Mathis et al., 2004.

The authors choose to use low nucleation exponents for sulfuric acid (in the range of 0.25 to 1) because they fitted best to the available measurement data and justify their choice based on their findings that classical nucleation theory may overstate the sulfuric acid nucleation exponent (Olin et al, 2014). One of their conclusions is that the values of nucleation exponent lower than unity suggest that other compounds such organics might have a significant role in the nucleation process. Is there any further evidence for such a claim? Other studies, etc.? To my knowledge, this is the first time that such a low nucleation exponent is proposed.

This discussion will be considered during the open discussion.

Page 5. Subchapter 2.1 (Fluid dynamics model) – the transport equation is not necessary. Information concerning CFD code could be given in the presentation of CFD-TUTEAM model that follows

The transport equation has not relevant information; therefore, it is not needed here.

The equation is removed, and the declarations of the quantities after it are moved to after the Eq. (1), in page 5, line 17.

Page 9, line 6, “[...] used with the following forms” – reference needed

References should be added there.

Two references are added there. Now the sentence reads:

“In atmospheric modeling studies, activation and kinetic type nucleation rates have been used with the following forms (Sihto et al., 2009; Paasonen et al., 2010)”

Page 12, lines 17-20, “Therefore, the main differences...” – explain-justify better the reason of the differences between the two experiments.

A clarification here is worthwhile.

In page 12, lines 14-22, the clarified part now reads:

“Both measurements were performed with the same engine with nearly the same measurement system. In the simulated measurements of Arnold et al. (2012) (indexed by A), fuel sulfur content was 6 ppm, but in the measurements of Rönkkö et al. (2013) (indexed by R), it was 36 ppm. The engine was equipped with a diesel oxidation catalyst (DOC) in both measurements, but there was a diesel particle filter (DPF) in A case and a partial diesel particle filter (pDPF) in R case. DPF reduces significantly more solid particles than pDPF. Therefore, the main differences between the results of these two experiments were slightly higher sulfuric acid concentrations in R case and the existence of solid particles in R case.”

Report in the discussion phase:

As I had pointed out in my review, the paper of Olin et al is a very interesting and useful for exploring mechanisms for nucleation events during diesel exhaust sampling. The revised version is even better, incorporating appropriately the comments. I found that the material that I recommended has been adequately included, making the whole work more reliable. I have not any additional comment; I think that the paper is very good.

Also the comment from the technical review phase which has not been taken into account yet:

“The authors choose to use low nucleation exponents for sulfuric acid (in the range of 0.25 to 1) because they fitted best to the available measurement data and justify their choice based on their findings that classical nucleation theory may overstate the sulfuric acid nucleation exponent (Olin et al, 2014). One of their conclusions is that the values of nucleation exponent lower than unity suggest that other compounds such organics might have a significant role in

the nucleation process. Is there any further evidence for such a claim? Other studies, etc.? To my knowledge, this is the first time that such a low nucleation exponent is proposed.”

is now taken into account in the manuscript. In the cases where the nucleation exponent is below unity, the first nucleation theorem would imply that the nucleated cluster contains less than one molecule of sulfuric acid; therefore, it seems that some other compounds are missing from the nucleation scheme. The organics were claimed due to their existence in the particles and due to the nucleation scheme tested by Pirjola et al. (2015), which has produced the most reliable results compared to the nucleation schemes without the organics. Another study claiming organics in the nucleation process is Riccobono et al. (2014). The corresponding text in the manuscript is now clarified.

Manuscript prepared for Atmos. Chem. Phys. Discuss.
with version 2014/09/16 7.15 Copernicus papers of the \LaTeX class copernicus.cls.
Date: 18 April 2015

CFD modeling of a vehicle exhaust laboratory sampling system: sulfur driven nucleation and growth in diluting diesel exhaust

M. Olin, T. Rönkkö, and M. Dal Maso

Aerosol Physics Laboratory, Department of Physics, Tampere University of Technology, P.O. Box
692, 33101 Tampere, Finland

Correspondence to: M. Olin (miska.olin@tut.fi)

Abstract

A new exhaust aerosol model CFD-TUTEAM (Tampere University of Technology Exhaust Aerosol Model for Computational Fluid Dynamics) was developed. ~~The model can be used to simulate particle formation and evolution in diesel exhaust~~ It is based on modal aerosol dynamics modeling with log-normal assumption of particle distributions. The model has an Eulerian sub-model ~~that provides~~ providing detailed spatial information within the computational domain, and a computationally less expensive, but spatial information-lacking, Lagrangian sub-model ~~that can be used to examine particle formation in a high temporal resolution.~~ Particle formation in a laboratory sampling system that includes a porous tube type diluter and an aging chamber was modeled with CFD-TUTEAM. The simulation results imply that over 99 % of new particles are formed in the aging chamber region, because nucleation rate remains at high level in the aging chamber due to low dilution ratio and low nucleation exponents. The nucleation exponents for sulfuric acid in sulfuric acid-water nucleation ranging from 0.25 to 1 appeared to fit best with measurement data, which are the same values as obtained from the slopes of the measured volatile nucleation mode number concentration vs. the measured raw exhaust sulfuric acid concentration ~~obtained from the measurement data.~~ These nucleation exponents are very low compared to the nucleation exponents obtained from the classical nucleation theory of binary sulfuric acid-water nucleation. The values of nucleation exponent lower than unity suggest that other compounds, such as hydrocarbons, might have a significant role in the nucleation process.

1 Introduction

Ultrafine particles are related to adverse health effects (Dockery et al., 1993; Pope et al., 2002; Beelen et al., 2014) and various effects on climate (Arneth et al., 2009). Diesel vehicles have cause a significant ~~role on the health effects~~ fraction of health effect-inducing exposure, because they have present a major contribution to ultrafine particles of urban air (Virtanen et al., 2006; Johansson et al., 2007; Pey et al., 2009) and because the sizes of

the particles emitted by diesel vehicles lie in the range of high lung deposition probability (Alföldy et al., 2009; Rissler et al., 2012).

Fuel combustion generates solid particles, such as soot, ash, core (Rönkkö et al., 2007), and nanosized carbonaceous particles (Sgro et al., 2008). In addition to solid particles, liquid particles are also formed. Unlike solid particles, liquid particles are formed after the combustion process during exhaust cooling (Kittelson, 1998). In the case of a vehicle, this occurs when the exhaust is released from the tailpipe. ~~These Liquid~~ particles are smaller ~~in size~~ than soot particles, and they are formed through nucleation process; thus, they are frequently called nucleation particles. ~~In fact, nucleation process~~ Strictly speaking, the nucleation process by definition involves an energy barrier, ~~but and it has been shown that~~ particle formation can be a barrierless process also (Vehkamäki and Ripinen, 2012). For simplicity, we call the particle formation process in this article ~~is called nucleation process~~ 'nucleation', whether it ~~has involves~~ an energy barrier or not.

~~Particle-The particle~~ size distribution controls ~~the~~ aerosol deposition to the respiratory system and its behavior in the atmosphere. Modeling studies can provide information on vehicle exhaust particle formation and evolution in the atmosphere. To model particle concentration and the size of nucleation mode, the actual nucleation rate ~~is required~~ needs to be known. ~~Modeling~~ In addition, modeling of vehicle exhaust particle formation can ~~provide useful information on the atmospheric nucleation also.~~

also provide insight on nucleation and particle formation processes in more dilute environments. The detailed nucleation mechanism ~~that controls controlling~~ particle formation in vehicle exhaust is currently unknown. ~~Nucleation particles are known to consist of~~ Studies have shown that nucleation particles contain at least water, sulfuric acid, and hydrocarbons (Kittelson, 1998; Tobias et al., 2001; Sakurai et al., 2003; Schneider et al., 2005), ~~and therefore;~~ therefore, it is likely that these could be involved in the nucleation process. Sulfuric acid vapor (also called 'gaseous sulfuric acid' in literature) concentration in diesel exhaust (Rönkkö et al., 2013), fuel sulfur content (Maricq et al., 2002; Vogt et al., 2003; Vaaraslahti et al., 2005; Kittelson et al., 2008), lubricating oil ~~sulfuric~~ sulfur content (Vaaraslahti et al., 2005; Kittelson et al., 2008), and exhaust after-treatment (Vogt et al.,

2003) have been found to correlate with nucleation particle concentration, at least in the cases when the test vehicle has been equipped with an oxidative exhaust after-treatment. ~~For an opposite example~~As a counter-example, no correlation between fuel sulfur content and particle number concentration can be seen from the results of Rönkkö et al. (2007).

Particle formation and dilution in vehicle exhaust and in laboratory sampling systems has been studied by several authors (Vouitsis et al., 2005; Lemmetty et al., 2006, 2008; Arnold et al., 2012; Li and Huang, 2012; Pirjola et al., 2015) in temporal coordinates. However, because particle formation in diluting vehicle emission involves strong gradients in temperature and the ~~concentration of~~concentrations of the compounds involved, full understanding of the particle formation process requires also information in ~~the~~ spatial dimensions, usually done by using a computational fluid dynamics (CFD) approach. For vehicle exhaust plumes, modeling efforts to elucidate this situation have ~~been undertaken recently~~recently been undertaken (Uhrner et al., 2007; Albriet et al., 2010; Liu et al., 2011; Wang and Zhang, 2012; Huang et al., 2014). These efforts, however, have focused on real-world dilution situations, for which boundary conditions are difficult to obtain. Controlled observations of vehicle emissions are usually performed in laboratory conditions involving diluting sampling systems. CFD modeling of particle formation in a perforated tube diluter (its operating principle corresponds to a porous tube diluter (PTD) used in exhaust laboratory measurements) with dibutylphthalate (DBP) has been performed by Pyykönen et al. (2007). To our knowledge, no CFD modeling studies involving realistic vehicle exhaust in realistic emission sampling situations have been performed.

In this paper, an exhaust aerosol model for application in CFD modeling of realistic vehicle exhaust and its applicability to study particle formation involving sulfuric acid in diesel exhaust using previously published data (Arnold et al., 2012; Rönkkö et al., 2013) are presented. Two versions of the model code, an Eulerian and a Lagrangian model, are presented. ~~Then the~~The Eulerian model can provide the spatial information inside the sampling system, but the Lagrangian model can be used with lower computational cost due to a lower dimensionality but it lacks spatial information. The Eulerian model is used to examine the spatial distribution of particle formation and growth in the modeled experimental setup,¹

findings in light of different possible nucleation mechanisms through the dependence of the formation rate on the sulfuric acid concentration are studied. In addition ~~it was possible to study the~~, model results enabled the study of relative rates of different aerosol ~~dynamical processes~~dynamics processes, such as coagulation and deposition, inside the sampling setup, which provides valuable information for future studies of vehicle emissions. Finally, because vehicle emission studies are used as input for modeling studies of atmospheric aerosol loading, the spatial information gained from our model gives insight into the applicability of emission studies for such upscaling purposes.

2 Model description

2.1 Fluid dynamics model

The CFD code used was a commercially available software ANSYS FLUENT 14.0. It can be used to solve, e.g., flow, mass, heat, and radiation transfer problems. It is based on finite volume method (ANSYS, 2011), where-in which the computational domain is divided into a finite amount of cells. Governing equations of the flow are solved in every computational cell iteratively until sufficient convergence is reached. In this case study, the governing equations are continuity, momentum, energy, turbulence, gas species, and aerosol scalars transport equations.

2.2 Aerosol dynamics model CFD-TUTEAM

~~Aerosol~~ The aerosol dynamics model CFD-TUTEAM (Tampere University of Technology Exhaust Aerosol Model for Computational Fluid Dynamics) is based on the former aerosol model TUTEAM (Lemmetty et al., 2008). CFD-TUTEAM models-represents aerosol distributions modally (Whitby and McMurry, 1997), i.e. the total distribution is divided into log-normally distributed modes of different particle sizesizes. A single-component mode j is modeled by three variables, which are number $M_{j,0}$, surface area $M_{j,2/3}$ and mass $M_{j,1}$ moment concentrations of a-the distribution. The concentration of a k th moment of a mode

j has a governing equation (Whitby and McMurry, 1997)

$$\frac{\partial M_{j,k}}{\partial t} = -\nabla \cdot (M_{j,k} \mathbf{u}) + \nabla \cdot \left(\rho_f \bar{D}_{j,k,\text{eff}} \nabla \frac{M_{j,k}}{\rho_f} \right) + \text{nucl}_{j,k} + \text{cond}_{j,k} + \text{coag}_{j,k}, \quad (1)$$

where \mathbf{u} is [the](#) flow velocity vector, ρ_f is [the](#) fluid density, $\bar{D}_{j,k,\text{eff}}$ is k th moment-weighted average of D_{eff} , and the last terms [present-represent](#) source terms for nucleation, condensation, and coagulation, which are described in Sect. 2.2.3. However, in [a](#) multi-component aerosol system, the mass moments are further divided into moments $M_{j,1,i}$ where i denotes a liquid component in the particle.

The parameters of log-normal distributions (number concentration N_j , count median diameter CMD_j and geometric SD GSD_j) can be [calculated-computed](#) from the three moments according to Whitby and McMurry (1997).

CFD-TUTEAM consists of an Eulerian and a [Lagrangian-type-Lagrangian-type](#) sub-model. In the Eulerian model, the moment variables are connected to the CFD model by solving the scalar transport equations of type Eq. (1). The Lagrangian model uses cooling and dilution profiles obtained from the CFD model as inputs.

2.2.1 Eulerian model

The Eulerian aerosol model is two-way coupled with the CFD model: (1) the properties on the fluid side affect on the transport equation of the particle variables Eq. (1); (2) nucleation and condensation on the aerosol side affect on the transport equation of gas species as negative source terms.

Temperature, gas species concentrations, and particle distribution parameters in hot exhaust and cold dilution air are the boundary conditions that are used at the domain boundaries in the corresponding inlets. Computation of the CFD model and the Eulerian aerosol model provide the solution for flow and particle parameters inside the simulation domain and their values at the outlet.

The simulation domain is a two-dimensional axial symmetric geometry. [A-The measurement setup to be modeled had no time-dependence in the results in a short](#)

time-scale, which allows a computationally more efficient steady-state simulation is performed, where all time derivatives are zero, which provides shorter computation timesimulation.

2.2.2 Lagrangian model

The Lagrangian aerosol model is a Matlab-code in which the differential equations Eq. (1), with the exception of the first two terms (convection and diffusion), are solved numerically. ~~The boundary conditions of temperature, gas species concentrations and particle distribution parameters are used as initial values.~~ Temperature and gas species concentration data from different path lines of the fluid obtained from the Eulerian CFD model are used as time series inputs for the Lagrangian model. The Lagrangian aerosol model is only one-way coupled with the CFD model, ~~but the influence of: gas-to-particle conversion (nucleation and condensation on the properties) has no effect on the fluid sideis negligible.~~

~~The calculation of the Lagrangian aerosol model provides the particle distribution parameters as a function of time for different path lines. The values at the ends of the different path lines can be averaged to get information on the particle parameters at the outlet. The one-way coupling approximation is sufficient as gas-to-particle conversion decreases the mass concentrations of sulfuric acid, water, and hydrocarbon vapors, in maximum, by 4 %, 1 %, and 1 %, respectively, in the whole simulation domain of the Eulerian simulations. The one-way coupling also enables the modeling of particle dynamics with a higher resolution compared to fluid modeling.~~

~~There is~~ The path lines contain no spatial information ~~at the path lines~~ in the Lagrangian model, but temporal information ~~exist~~exist. However, the Lagrangian model ~~is also considered as~~ can also be considered a steady-state simulation, because the inputs are obtained from a steady-state CFD simulation. Due to fewer dimensions in the Lagrangian model compared to the Eulerian model, a very high temporal resolution can be simulated. ~~That can be used to ensure the sufficiency of spatial resolution of the computational grid of with the same computational cost. The output from the Eulerian model is actually interpolated to a higher resolution to match the input required for the~~

Lagrangian model. However, the Lagrangian model has, in principle, the same resolution for temperature and gas species concentrations as the Eulerian model by comparing the because the solution has been calculated using the lower resolution. The higher resolution is, however, used for particle dynamics in the Lagrangian model. Therefore, comparing the particle distribution results from both models provides information on the sufficiency of the spatial resolution of the Eulerian model. A high resolution is required for particle dynamics processing due to the non-linear and exponential nature of the equations controlling particle dynamics.

Running the Lagrangian aerosol model provides the particle distribution parameters as a function of time for different path lines. The values at the ends of the different path lines can be averaged to get information on the particle parameters at the outlet.

2.2.3 Aerosol dynamics

Modeled aerosol processes are shown in Fig. 2, and different terms of Eq. (1) are explained next.

“Nucleation” is a key process controlling particle number concentration in diluting exhaust ~~is~~ particle formation, which is generally considered sulfur-driven, more specifically sulfuric acid-driven. Binary homogeneous nucleation (BHN) of water and sulfuric acid has been used as a nucleation mechanism in previous diesel exhaust modeling studies (Lemmetty et al., 2006, 2008; Uhrner et al., 2007; Albriet et al., 2010; Liu et al., 2011; Li and Huang, 2012; Wang and Zhang, 2012; Huang et al., 2014). The nucleation rate J of BHN can be derived from classical thermodynamics, and the theory for this is called classical nucleation theory (CNT). Following the first nucleation theorem (Kashchiev, 1982), the nucleation exponent for nucleating species i is defined as:

$$n_i = \frac{\partial \log J}{\partial \log C_i}, \quad (2)$$

where C_i is the concentration of species i . According to CNT, the nucleation exponent for ~~gaseous sulfuric acid~~ sulfuric acid vapor (subscript: sa) n_{sa} in vehicle exhaust is

about 5 or more. In activation type nucleation (Kulmala et al., 2006), $n_{sa} = 1$, and in kinetic nucleation (McMurry and Friedlander, 1979), $n_{sa} = 2$. Nucleation exponents 1 and 2 are found to fit to atmospheric measurement results better than the values from CNT in some studies (Sihto et al., 2009), but they higher than 2 have also been observed (Wang et al., 2011; Herrmann et al., 2014). However, nucleation exponents have not yet been widely explored in connection with diesel exhaust. The nucleation mechanism in diesel exhaust can differ from the mechanism in atmosphere due to different gas concentration and temperature rangeranges. According to our simulations with CNT nucleation (Olin et al., 2014), nucleation rate obtained from CNT needs to be corrected with a relatively large factor that decreases exponentially (correction factor $\propto [H_2SO_4]^{-6.6}$) with increasing sulfuric acid concentration (Fig. 1). This result suggests that CNT may overestimate n_{sa} with a value of 6.6. Therefore, n_{sa} in diesel exhaust could be very low. Low nucleation exponents indicate that there may be other species, such as organic compounds, that also take part in the nucleation process. Paasonen et al. (2010) have modeled different nucleation mechanisms, including organic nucleation mechanisms, for background atmospheric conditions, and have observed that they correlate with measurement data better than sulfur driven nucleation in some cases. Mathis et al. (2004a) have experimentally determined that some organic compounds are being capable of initiating and increasing or decreasing (depending on the functional groups) nucleation mode particles-particle concentration emitted by a diesel engine.

However, the actual nucleation rate, which is the rate of the formation of new stable molecule clusters (Vehkamäki and Riipinen, 2012), cannot was not able to be measured directly, until recently before the launch of, e.g., Airmodus PSM (Vanhanen et al., 2011), due to the small sizes of the clusters. The measurable quantity is the concentration of particles that are large enough for measurement devices, of which the observed nucleation rate can be estimated. Particle dynamics, such as condensation and coagulation, alter the particle distribution during the time, when newly formed clusters grow to measurable sizes. Therefore, the actual and, from which the observed nucleation rates are unequal and their nucleation exponents can be different too exponent can be calculated but not the actual one.

In atmospheric modeling studies, activation and kinetic type nucleation rates have been used with in the following forms (Sihto et al., 2009; Paasonen et al., 2010)

$$J_{\text{act}} = A[\text{H}_2\text{SO}_4] \quad (3)$$

$$J_{\text{kin}} = K[\text{H}_2\text{SO}_4]^2, \quad (4)$$

where A and K are activation and kinetic coefficients, respectively. The coefficients A and K are currently empirical constants fitted from experimental data in atmospheric modeling studies. Constant coefficients can be satisfactory approximations in atmospheric nucleation experiments, where temperature T and relative humidity RH remain nearly constants. In contrast, T and RH in vehicle exhaust are varying highly variable during the dilution and cooling process. Laboratory (Mathis et al., 2004b) and on-road studies (Rönkkö et al., 2006) of diesel exhaust particle emissions suggest that T and RH affect the nucleation particle concentration; thus, T and RH have a role in are involved in determining the nucleation rate. Therefore, constant coefficients cannot be used in modeling particle formation in vehicle exhaust.

Nucleation The nucleation term in Eq. (1) is only related to the volatile nucleation mode (subscript: vol), and for different moments it is

$$\text{nucl}_{\text{vol},0} = J$$

$$\text{nucl}_{\text{vol},2/3} = Jm^{*2/3}, \quad (5)$$

$$\text{nucl}_{\text{vol},1,i} = Jm_i^*$$

where m^* is the mass of the cluster formed by nucleation and m_i^* the mass of component i in the cluster. Nucleation The nucleation rate J depends on the theory used. In this case study, the following nucleation scheme is used:

$$J = \frac{k_{n_{\text{sa}},n_w}}{p_{\text{sa}}^\circ(T)} [\text{H}_2\text{SO}_4]^{n_{\text{sa}}} [\text{H}_2\text{O}]^{n_w}, \quad (6)$$

where k_{n_{sa},n_w} is a proportionality constant and p_{sa}° is the saturation vapor pressure of sulfuric acid that can be found from Kulmala and Laaksonen (1990). This scheme was

selected because it is the simplest form of a nucleation scheme where the dependencies of sulfuric acid and water vapors and temperature are included. In this form, the roles of T and RH have been included into ~~the~~ nucleation rate by an ad hoc formulation. ~~Temperature~~ The temperature dependency has been included through p_{sa}° , ~~and it due to the exponential temperature-dependency of p_{sa}° , which has been found to be the case also for experimentally determined nucleation rates (Wölk et al., 2001; Iland et al., 2004)~~. p_{sa}° is in the ~~divisor denominator~~ because increasing temperature has a decreasing effect on nucleation rate. The dependency of ~~the nucleation rate on~~ RH ~~on nucleation rate~~ is included through ~~water the water vapor~~ concentration and the nucleation exponent of it (~~n_w same way~~) in the same manner as for sulfuric acid. In the ~~situation case~~ of constant T and RH, the nucleation rate Eq. (6) ~~would reduce reduces~~ to a form of Eq. (3) ~~in the case of if the nucleation exponent is~~ $n_{\text{sa}} = 1$.

“Condensation” in the model is assumed to occur by sulfuric acid, water ~~and hydrocarbons~~. ~~Condensation~~, ~~and hydrocarbon vapors~~. The ~~condensation~~ term for sulfuric acid is

$$\text{cond}_{j,1,\text{sa}} = \int_{-\infty}^{\infty} \frac{\partial m_{\text{p},j,\text{sa}}}{\partial t} \frac{dN}{d \ln d_{\text{p}}} d \ln d_{\text{p}}, \quad (7)$$

where $\frac{\partial m_{\text{p},j,\text{sa}}}{\partial t}$ is the mass growth rate of ~~a~~ single particle in mode j of diameter d_{p} by sulfuric acid, described in Appendix A, and $\frac{dN}{d \ln d_{\text{p}}}$ is the density function of ~~the~~ log-normal distribution. Because water condensation and evaporation are very fast processes for small particles in low RH (Wilck, 1998), modeling them would require ~~a~~ very dense computational grid. Therefore, the water content in the equilibrium state of particles is computed following the approach of Uhrner et al. (2007), but with an additional iterative equilibrium checking procedure described in Appendix A. ~~Condensation~~ ~~The condensation~~ term for water be-

comes

$$\text{cond}_{j,1,w} = \kappa_j \frac{Y_{j,w}^{\text{eq}}}{Y_{j,\text{sa}}^{\text{eq}}} \text{cond}_{j,1,\text{sa}}, \quad (8)$$

where κ_j is a factor for water equilibrium, $Y_{j,w}^{\text{eq}}$ and $Y_{j,\text{sa}}^{\text{eq}}$ are the mass fractions of water and sulfuric acid in a particle that is in water equilibrium. Two immiscible liquid phases are considered in the particles: (1) solution of sulfuric acid and water, (2) a hydrocarbon mixture. ~~Condensation~~ The condensation term for hydrocarbons is of the form of Eq. (7), but with an additional factor f_{hc} ~~that is considered as~~ considered to be the fraction of hydrocarbons able to condense at temperature T . The phase interactions and the hydrocarbon fraction are described in Appendix A. Due to the decreasing ~~trend of temperature~~ temperature trend in the simulations of the sampling system, no evaporation process is included in the model.

“Coagulation” modeling is based on the model of Whitby and McMurry (1997). Intramodal coagulation of the volatile nucleation mode and intermodal coagulation from the volatile nucleation mode to ~~the~~ other modes are modeled (Fig. 2). The modeling of intramodal coagulation of the core and soot modes and intermodal coagulation between them are neglected due to their insignificance and irrelevancy ~~of them~~ compared to the ~~modeled~~ other coagulation directions.

“Diffusion” is modeled as laminar and turbulent parts. The laminar diffusion coefficient for particles $D_{p,\text{lam}}$ is expressed ~~as with the~~ Stokes–Einstein relation (Hinds, 1999)

$$D_{p,\text{lam}} = \frac{k_B T C_c(d_p)}{3\pi\mu_f d_p}, \quad (9)$$

where k_B is the Boltzmann constant, C_c is the slip correction coefficient (Allen and Raabe, 1985), μ_f is the dynamic viscosity of the fluid, and d_p is the particle diameter. The turbulent diffusion coefficient D_t is computed as $D_t = \nu_t / \text{Sc}_t$ where ν_t is the kinematic viscosity of the fluid, and Sc_t is the turbulent Schmidt number, for which the default value of 0.7 is used. The effective diffusion ~~coefficient of coefficients of the~~ gas species and of particles are $D_{\phi,\text{eff}} = D_{\phi,\text{lam}} + D_t$. In the Lagrangian model, diffusion is not modeled as in the Eulerian

model ~~–In this case, diffusion due to the lack of particle concentration gradients.~~ In the Lagrangian model, diffusion outflux from a path line is seen as dilution of gas species and particles, which is modeled using the following formula:

$$M_{j,k}(t + \Delta t) = M_{j,k}(t) \frac{DR(t)}{DR(t + \Delta t)}, \quad (10)$$

where DR denotes the dilution ratio. The dilution profiles are obtained from the CFD simulation. However, the diffusion influx to the path line from the surrounding areas cannot be modeled with the Lagrangian model due to lower dimensionality.

“Deposition” onto the surfaces is assumed to occur only due to diffusion, because thermophoresis is was found to have only a minor ~~effect to deposition because of role on deposition due to~~ low thermal gradients. Deposition is modeled by setting all moments to zero on the walls.

3 Simulation setup

3.1 Simulated experiments

To demonstrate the applicability of the CFD-TUTEAM, we applied it to a laboratory sampling system for which data has already been published by Arnold et al. (2012) and Rönkkö et al. (2013). These experiments were chosen due to the availability of simultaneous measurements of particle number concentration, size distributions, and gas-phase sulfuric acid concentrations. The experiments were performed at the engine dynamometer for a heavy-duty diesel engine. The exhaust sampling was performed with a modified partial flow sampling system (Ntziachristos et al., 2004) seen in Fig. 3. It consists of a PTD, an aging chamber and ejector diluters. It is used to mimic the particle formation of a real-world driving situation in a laboratory-scale measurement (Keskinen and Rönkkö, 2010).

In both measurements (Arnold et al., 2012; Rönkkö et al., 2013), ~~gaseous-sulfuric acid~~ sulfuric acid vapor concentration before the sampling system and particle distribution after the sampling system were measured. Both measurements were performed with the

same engine with nearly the same measurement system. In the simulated measurements of Arnold et al. (2012) (indexed by A), fuel sulfur content was 6 ppm, but in the measurements of Rönkkö et al. (2013) (indexed by R), it was 36 ppm. The engine was equipped with a diesel oxidation catalyst (DOC) in both measurements, but there was a diesel particle filter (DPF) in ~~A-case~~ case A and a partial diesel particle filter (pDPF) in ~~R-case~~. ~~DPF reduces significantly more solid particles than pDPF~~ case R. A DPF reduces the number of solid particles significantly more than a DPF. Therefore, the main differences between the results of these two experiments were slightly higher (~ 50 % in maximum sulfuric acid cases) sulfuric acid concentrations in the R case and the existence of solid particles in the R case.

~~Measurements of~~ The measurements performed with 100 % engine load of the steady driving mode were simulated. ~~Volatile nucleation mode concentration increased in both measurements, when sulfuric acid concentration increased over the time, though all the operation parameters remained constant~~ All the operation parameters remained constant during the measurement points, but the sulfuric acid vapor concentration increased slowly while the time elapsed due to the unsteadiness of the storage effect of the after-treatment system (Arnold et al., 2012; Rönkkö et al., 2013) . As the sulfuric acid vapor concentration was increasing, also the volatile nucleation mode concentration was increasing.

3.2 Computational domain

The ~~computational domain for the simulations consisted of PTD and aging chamber only. Secondary dilution, such as ejector diluters, is~~ sampling system seen in Fig. 3 consists of a PTD, an aging chamber, and an ejector diluter. Ejector diluters are used to stop the aerosol processes that alter the particle distribution, and to obtain the conditions of the sample required for measurement devices. According to the measurements of Lyyränen et al. (2004) and Giechaskiel et al. (2009), an ejector diluter has only a minor effect on the nucleation mode particle concentration. Particle ~~Therefore, particle~~ distribution at the outlet of aging chamber is considered here can be considered the measured particle distribution, though the ~~particle distribution was measured~~ measurements were done after the ejector

~~diluters in the experiments. The axial symmetric domain is presented in diluter in reality. The computational domain for the simulations (Fig. 4) was selected to consist of the PTD and the aging chamber only.~~

The domain ~~is was~~ divided into ~ 0.5 million computational cells, of which the major part ~~are were~~ located inside the PTD where the smallest cells are needed due to ~~high the highest~~ gradients. The smallest cells ~~are were~~ $5\ \mu\text{m}$ in side lengths and ~~are were~~ located in the beginning of the porous section, where the hot exhaust and the cold dilution air ~~encounter meet~~.

Internal fluid ~~is was modeled as~~ a mixture of air, water vapor, ~~gaseous sulfuric acid, and sulfuric acid vapor, and the~~ hydrocarbon mixture. Particle scalars ~~are within internal fluid also, but are were also within the internal fluid, but were~~ not connected to ~~the~~ fluid properties. ~~External fluid is The external fluid was~~ modeled as air, ~~the~~ insulation zone as wool, and the solid zones of the PTD and the aging chamber as steel.

3.3 Boundary conditions and simulation parameters

The boundary conditions are described in Table 1. 8 cases from Rönkkö et al. (2013) measurements and 9 cases from Arnold et al. (2012) measurements with different sulfuric acid ~~vapor~~ mole fractions were simulated. For R cases, nonvolatile nucleation mode (core mode, subscript: core) and soot mode (subscript: soot) concentrations vary depending on the case. For A cases, core and soot modes were not ~~found; and therefore, observed, and they were therefore~~ omitted from the simulations. Other parameters ~~remain remained~~ nearly constants in different cases.

~~Water The water~~ vapor mole fraction in exhaust was calculated from ~~the~~ combustion reaction stoichiometry and with ~~lambda value a lambda value (the fraction of injected air mass compared to the air mass required for the stoichiometric combustion) of~~ 1.54. ~~Water vapor The water vapor concentration~~ in dilution air was obtained by assuming that dilution air RH was 10 %. RH was not measured, but RH = 10 % can be considered an upper limit, ~~because the pressure of the compressed air (maximum RH is 100 %) used for the dilution air was 10~~ bar. Total hydrocarbon mole ~~fraction (except for fractions (except the most~~ volatile

hydrocarbons) ~~was fitted to obtain in the raw exhaust were set to values that produce~~ the measured volatile nucleation mode particle sizes ~~(the diameter of a particle with the average volume) at the outlet.~~

Deposition ~~was implemented~~ in the CFD model ~~was implemented~~ by setting the mole fraction ~~for a depositing vapor~~ at the boundary to zero ~~for a depositing gas~~; for non-depositing ~~gas vapor~~, a zero flux at the boundary was implemented. ~~Gas is~~ ~~A vapor was~~ considered depositing, if its saturation ratio ~~exceeds unity at~~ ~~exceeded unity near~~ the boundary, and non-depositing otherwise. For sulfuric acid ~~vapor~~, saturation never exceeded unity in these simulations; hence ~~zero flux~~ ~~the zero flux assumption~~ was always used. In reality, dilution air cools ~~PTD, but the cooling is not simulated here. Therefore, the PTD;~~ ~~however, the cooling was not simulated because it would require the modeling of the dilution air outside the dilution air inlet boundary. This would have increased the complexity of the simulation due to the porousness of the diluter and due to the requirement for a 3-D simulation. We estimate that~~ exhaust temperatures in the sampling pipe of ~~PTD would then~~ ~~the PTD would~~ be lower and ~~the~~ dilution air temperatures higher near the boundary where ~~the~~ hot exhaust and cold dilution air ~~encounter~~ ~~are mixed~~. Hence, sulfuric acid ~~might then be condensed~~ ~~vapor might condense~~ on the cooled inner walls of the sampling pipe of ~~PTD. Saturation ratio of over the PTD. A saturation ratio of more than~~ unity for hydrocarbons was calculated as a fraction of condensing hydrocarbons f_{hc} described in Appendix A. All particles were modeled as depositing; thus, all moments were set to zero on the walls.

For ~~the~~ volatile nucleation mode, GSD_{vol} was ~~let to vary~~ ~~varied~~ between 1 ~~and~~ 2 to ensure it ~~to remain~~ ~~remaining~~ in a reasonable range. Nucleation produces ~~a~~ monodisperse particle distribution, ~~of for~~ which GSD is 1, if a constant cluster size is used. The measured values of GSD_{vol} after the aging chamber were in the range of between 1.2 and 1.3. For ~~the~~ core and soot modes, constant values $GSD_{core} = \sim 1.13$ and $GSD_{soot} = 2.16$ were used, ~~which correspond to the~~ ~~corresponding to~~ measured values. Hence, the surface moments for ~~the~~ core and soot modes could be omitted from the model. ~~Core mode had initially~~ ~~$CMD_{core} = 10\text{ nm solid particle}$~~ ~~The core mode was initially a solid particle~~ ~~($CMD_{core} = 10\text{ nm}$)~~ distribution, onto which ~~liquids condense and coagulate. Soot vapors~~

could condense and which are coagulated with volatile nucleation mode particles. The soot mode was modeled as ~~spherical particle distribution~~ a distribution of spherical particles with a constant CMD_{soot} of 49 nm, which is the measured CMD of the mobility diameter of soot particles. The ~~reason for reasoning behind~~ using a constant value was due to the assumption, based on measurements, that soot particles do not grow by condensation ~~but gases condense into~~, but instead vapors condense into the empty spaces of the fractal particles (Lemmetty et al., 2008). Therefore, the mobility diameter remains constant, but the effective density increases. The value of $\rho_{\text{soot}} = 380 \text{ kg m}^{-3}$ was used as the effective density of a dry soot particle (Virtanen et al., 2002), assuming 49 nm particle with the fractal dimension of 2.5 and the primary particle diameter of 5 nm. The validity of the assumption was tested by calculating the mobility diameter in the case where condensation is most dominant: if all the empty spaces of the fractal particles were filled with the condensing vapors and the coagulation from the volatile nucleation mode were taken into account, CMD_{soot} would increase to the value of about 60 nm in maximum. Therefore, the assumption that CMD_{soot} remains as the value of 49 nm could be a valid approximation.

Due to steady-state simulations, all governing equations were Reynolds-averaged, i.e. time-averaged. The averaging of the momentum transport equations causes additional terms, called Reynolds stresses, to appear. Turbulence models are used to model the Reynolds stresses, but the calibration of the turbulence models ~~have has~~ been done with experimental data, and the calibration may not be suitable in cases with different geometries, fluid mixture, and boundary conditions. In this case, SST- $k-\omega$ with ~~Low-Re~~ low-Re correction (ANSYS, 2011) was used as a turbulence model. It produced the most reliable results of the available turbulence models using Reynolds stresses, ~~according to pressure drop during~~ based on the pressure drop in the porous section. ~~Modeled~~ The modeled turbulence levels have, however, a high influence on the results, mainly on the deposition rates: an overestimated turbulence level will overestimate deposition rates and the output particle concentrations will, therefore, be underestimated. Particle concentration measurements in both boundaries of the simulation domain would have provided advantageous information on validating the turbulence model for this case, but that kind of measurement has not yet

been done. Enhanced turbulence models, such as Large Eddy Simulation (LES) or Direct Numerical Simulation (DNS), could produce more reliable results, but the computational cost of them is significantly higher compared to Reynolds stress models.

All cases were simulated with two nucleation exponents for sulfuric acid vapor: $n_{sa} = 0.25$ and $n_{sa} = 1$. Relatively low nucleation exponents were chosen due to our findings (Olin et al., 2014) that imply previous findings (Olin et al., 2014) implying that the nucleation exponents obtained from CNT are too high. ~~Nucleation~~ The nucleation exponent for water vapor n_w was assumed to be unity in all cases, due to the lack of detailed information on that. ~~Therefore~~ specifying otherwise. Thus, the nucleation rates used were the following:

$$J = \frac{5.01 \times 10^{-15} \text{ Pa cm}^{0.75} \text{ s}^{-1}}{p_{sa}^{\circ}(T)} [\text{H}_2\text{SO}_4]^{0.25} [\text{H}_2\text{O}] \quad (11)$$

$$J = \frac{7.63 \times 10^{-23} \text{ Pa cm}^3 \text{ s}^{-1}}{p_{sa}^{\circ}(T)} [\text{H}_2\text{SO}_4] [\text{H}_2\text{O}], \quad (12)$$

where the units are $\text{cm}^{-3} \text{ s}^{-1}$, Pa, and cm^{-3} for nucleation rate, vapor pressure and, and vapor concentrations, respectively. The proportionality constants were chosen by fitting the simulated particle concentrations with the measured ones. According to the first nucleation theorem (Kashchiev, 1982), the composition of the critical cluster is connected to the nucleation exponents. However, the composition of a newly formed particle newly formed particles did not follow the first nucleation theorem in this case, because, firstly, nucleation exponents lower than unity would lead to a cluster containing indiscrete amount of molecules. Secondly, the critical cluster composition and nucleation exponents have recently been found to be unconnected (Kupiainen-Määttä et al., 2014). Therefore, we chose to define the newly formed particle was chosen to be defined as a particle with a diameter of 1.5 nm, which is a relevant size of a particle from which atmospheric aerosol formation starts (Kulmala et al., 2007). However, the atmospherically relevant size may not be simply transferred to the clearly different conditions (such as temperature and vapor concentrations) prevailing in vehicle exhaust, but it is used here due to a lack of detailed information on that. A particle of that size would have the estimated size would need to

contain 15 sulfuric acid and 20 water molecules to remain in water equilibrium in temperature of 100 °C and RH of 10 %. Hence, the cluster formed by nucleation had the following masses of the components:

$$m_{sa}^* = 15 \times \frac{98.079 \text{ g mol}^{-1}}{N_A}$$

$$m_w^* = 20 \times \frac{18.015 \text{ g mol}^{-1}}{N_A}, \quad (13)$$

where N_A is the Avogadro constant.

4 Results and discussion

4.1 Spatial examination of particle formation in the sampling system

Figures ~~?? and ??~~ 5 and 6 show that nucleation begins at the boundary of where the hot exhaust and the cold dilution air ~~-.With-meet.~~ With a higher nucleation exponent n_{sa} , the nucleation rate reaches higher maximum values, but it also diminishes faster. This can be seen clearer from Fig. 7 where the nucleation rate with the nucleation exponent of unity has a higher maximum also on the axis and it decreases faster compared to the nucleation exponent of 0.25. Due to low nucleation exponents and a low dilution ratio $DR = 12$, the nucleation rate remains high in the aging chamber, where the dilution process has already finished. According to the simulations, over 99 % of the particles were formed in the aging chamber in all cases, which can be seen from Fig. 8 where the volatile nucleation mode concentration increases approximately two orders of magnitude during the aging chamber.

In R cases, the volatile nucleation mode number concentration was decreased by 3–9 % due to coagulation, depending on the case. Cases with the smallest particles had the highest coagulation losses due to ~~increased coagulation coefficient~~ higher coagulation coefficients. Coagulation to the soot mode contributed over 70 % of the total coagulation loss. Deposition onto the inner surfaces of ~~PTD and the PTD and the~~ aging chamber decreased the volatile nucleation mode concentration by 8–14 %, depending on the case.

Cases with the smallest particles had also the highest deposition losses due to the increased diffusion coefficient. About 25 % of core and soot particles were deposited. The fraction of the deposited particles was lower for the volatile nucleation mode, because the major depositing region is the expander in-at the beginning of the aging chamber (due to increased turbulence), where only a small fraction of all volatile nucleation mode particles ~~was already formed had been formed already~~.

Figures 9 and 10 present CMD for the volatile and nonvolatile nucleation modes in the aging chamber region. ~~GMD_{vol} at the outlet in R cases was obtained by fitting simulated and measured diameters of average volume with the amount of hydrocarbons in raw exhaust.~~ Values of CMD_{vol} are about 1 nm lower than measured (Fig. 11), because modeled GSD_{vol} values are higher (around 1.5) than measured (below 1.3). The error is probably caused by the simultaneous nucleation and condensation processes, which both ~~account in~~ affect the volatile nucleation mode distribution ~~that~~, which is modeled as log-normal in this model. In reality, the distribution will not remain log-normal when nucleation and condensation occur simultaneously.

Modeled values of CMD_{core} are about 4 nm higher than measured. This could be due to ~~underestimated overestimated dry~~ solid core particle size or underestimated condensation-Particle, or overestimated condensation to the nonvolatile nucleation mode. The particle distribution was not, however, measured after the aging chamber, but after the ejector ~~diluters that were diluter which was~~ omitted from the model. Because particle sizes can, in principle, increase also in ~~ejector diluters, the ejector diluter, the measured~~ CMD_{core} might be higher, if ejector diluters are modeled. However, values might be slightly lower, if the measurement would have been done before the ejector diluter. In that case, the measured CMD_{vol} would increase then, but not with as fast growth rate as values would be decreased more than CMD_{core} ; values due to smaller particle size because of the inversely proportionality of the growth rate to the particle size. Therefore, modeled values for the both CMD might be overestimated, and thus scaling of the hydrocarbon amount could reduce the discrepancy between the modeled and the measured values.

The required hydrocarbon vapor amount is also shown in Fig. 11, from which it can be seen that an increased amount of hydrocarbons-hydrocarbon vapors was required with increasing sulfuric acid amount. This is in correspondence vapor concentration. This corresponds with the observation of Arnold et al. (2012): the amount of acidic gases-vapors other than sulfuric acid correlates with the amount of sulfuric acid vapor. These acidic gases-vapors are mainly organic gases-vapors that have lower saturation vapor pressures compared to alkanes. Due to increased amount of low-volatile hydrocarbonshydrocarbon vapors, the fraction of condensing hydrocarbons-hydrocarbon vapors would be increased, but because the change of the composition of hydrocarbon mixture was not modeled, higher total hydrocarbon vapor amount was required. For A cases, a constant value of 3 ppmC₁ was used for hydrocarbon vapor amount, which produced CMD_{vol} values between 4.8 and 5.2 nm.

In A cases with $n_{sa} = 1$, only 0.5–4 % of sulfuric acid vapor condensed onto the particle phase (Table 2), but in R cases with $n_{sa} = 0.25$, about 80 % condensed. The difference is caused by the condensation sinks of solid particles, mainly due to the soot mode. Table 3 presents-shows the composition of the liquid-parts-liquid-phase compounds present in the particles, which are in agreement with the results of Pirjola et al. (2015), with the exception of the water content, which is approximately the half of the water content in the results of Pirjola et al. (2015). Hydrocarbons dominate the particle mass in the cases of lower raw exhaust sulfuric acid vapor concentrations. Table 3 also shows the maximum saturation vapor pressures of the hydrocarbons that are condensed onto the gas-particle phase. The values correspond to low-volatile or semi-volatile organic compounds.

In reality, the shape of the region of highest nucleation rates would be different and probably transferred towards the inner wall of the sampling pipe of the PTD due to the cooling of exhaust gas by dilution air that is not modeled here, which was not modeled. DBP nucleation simulations of Pyykönen et al. (2007) show that nucleation occurs in two regions: (1) right before the perforated section, and (2) during the perforated section. If nucleation exponents are higher in reality, nucleation rate will diminish steeply in the PTD region; therefore, the major part of nucleation will occur in-would occur in the PTD region. This could be examined

by measuring particle concentrations inside the aging chamber or with aging chambers of different lengths. If the major part of nucleation occurs in the aging chamber, it is not obvious that the nucleation process will be ~~stopped~~ quenched inside the secondary dilution. The position of nucleation region is also dependent on the effects of T and RH, but they cannot be observed from these simulations. Further investigations, where T and RH ~~will be changed and particle concentration will be~~ are varied and particle concentrations measured, are required to examine ~~the influence of them~~ these effects.

4.2 Comparison between Eulerian and Lagrangian models

A simulation performed by the Eulerian model of A case with raw exhaust sulfuric acid vapor concentration of $4.6 \times 10^{10} \text{ cm}^{-3}$ and with the nucleation exponent $n_{\text{sa}} = 1$ was modeled with the Lagrangian model also. The simulations ~~was done on three~~ were done for two path lines shown in Fig. ??, ~~from which temperature profile and gas~~ 7. Temperature, gas species concentrations, and particle dilution profiles as a function of time were exported from the ~~GFD model~~ Eulerian CFD model on the path lines. The blue path ~~starts~~ begins near the inner wall of the sampling tube, ~~and the red path near the axis,~~ and the green path between them. Due to cylindrical symmetry, the blue path has ~~the highest~~ a higher relevance on the output particle flux ~~and compared to~~ the red path ~~the lowest~~. ~~All the three lines have the~~. Both lines have a total residence time of about 1.6 s. The time domain was divided ~~to into~~ into 10^6 time steps, ~~which corresponds to a~~ resulting in a much higher resolution compared to the Eulerian simulation, ~~where in which~~ the paths pass through 6000–8000 computational cells.

Figure 12 ~~presents~~ shows the nucleation rates and the particle concentrations ~~on the three~~ along the path lines. The nucleation rate on the blue path develops slower ~~compared to the green and the red paths~~ than on the red path. That is because the blue path travels near the wall, thus the velocity is lower due to friction, ~~and~~. 21 ms ~~is~~ are required to reach the mixing region, which is a longer time than for the red path (7 ms) ~~and the green (8) paths~~. ~~In fact~~. In spatial coordinates, the nucleation rate on the blue path develops ~~fastest in spatial coordinates; because the blue path is the nearest path~~ closer to

the start, because it is nearer to the boundary where the hot exhaust and the cold dilution air ~~encounter, where meet, and the~~ nucleation rate has the highest values. For the times when the path lines are inside the mixing region, some fluctuations in the nucleation rate and in the particle concentration are seen, especially on the blue path. The fluctuations are caused by transition from the laminar exhaust flow to a turbulent flow as the dilution air accelerates the flow. The fluctuation of variables can be seen also in Figs. 5 and 6 at the end of the porous section.

Comparing the particle concentrations between the Eulerian and the Lagrangian simulations, it can be observed that the concentrations in the Eulerian simulations are higher in the beginning. That is caused by the diffusion influx of the particles from the surrounding areas of a path, which cannot be modeled with the Lagrangian model but is modeled in the Eulerian model. ~~The highest particle concentrations are on the cold side of the blue path; hence, the diffusion transports particles onto the location of the three paths. However, region where~~ the particle concentration jumps rapidly to a high level is the expander region of the aging chamber. The diffusion influx to the paths in that region can be seen in Fig. 13, which shows the particle concentration in the case where turbulent diffusion has been omitted. Omitting turbulent diffusion shows that a high particle concentration is formed in the expander due to a lower flow velocity in that section, which corresponds to a higher residence time. Because the Lagrangian model cannot model the diffusion influx from the high concentration area, the particle concentration remains lower in ~~the difference of the concentrations can also be partially accounted for numerical error caused by the lower resolution in the Eulerian simulation.~~ model. When turbulent diffusion is modeled, high turbulence in the expander region transfers particles in all directions, which is seen as flattened particle concentration fields as seen in Fig. 8.

The concentrations at the ends of all the paths are, however, almost the same, except for 20 % higher lower values in the Eulerian-Lagrangian simulation. The concentrations develop ~~to same values, nearly to the same values~~ because the major part of the nucleation occurs in the aging chamber where ~~every path experiences~~ the paths experience almost the same nucleation rates.

It can be seen from Fig. 14 that some ~~numerical error exists at the time when nucleation starts~~ fluctuations exist in CMD and GSD values in the Eulerian simulation, ~~which can be seen as a noise in CMD and GSD values. In as in~~ the case of ~~the Lagrangian simulation;~~ these values develop more smoothly through the time domain nucleation rate and particle concentration. The same time delay of the values on the blue path as for the nucleation rate can also be seen for CMD and GSD values. ~~Due to the diffusion~~ The jumps to higher values of CMD and GSD in the Eulerian simulation ~~that mixes particles of different size from the surrounding areas of the paths with the path areas, the particle distributions become wider, which can be seen as increased~~ are also caused by the diffusion influx from the expander region. Figure 15 presents CMD for the case of no turbulent diffusion. Due to a higher residence time in the expander region, particles grow larger; hence, a flow of larger particles by diffusion from the expander region to the path line area occurs. Adding larger particles rapidly to the initial particle distribution formed by nucleation causes rapidly increasing CMD and GSD values ~~compared to the values from the Lagrangian simulation~~. At the end, all GSD values approach nearly the same value, but CMD values appear to be about 0.5 nm lower in the Lagrangian simulation during the whole time domain.

Although the behavior of the Eulerian model during the fluctuating flow is not very smooth, the model is capable of approaching realistic values after that region. The fluctuation behavior can probably be smoothed by increasing the spatial resolution in that region. However, the values at the inlet and the outlets are of the main interest in this study; therefore, as the modeled outlet values for both models are approximately the same, the spatial resolution may be sufficient.

The Lagrangian model ~~appear~~ appears to produce almost equal results compared to the Eulerian model, if the output particle distribution is of interest only, despite the path line chosen ~~to be simulated. It for the simulation. However, in the inner areas of the sampling system, the Lagrangian model may produce unrealistic results if diffusion fluxes have strong effects on the particle distribution, which is especially seen in a turbulent flow. The Lagrangian model~~ can be executed with very high time resolution without being computationally expensive. However, it requires cooling and dilution profiles obtained from the

CFD model, if proper results are required. Additionally, the coupling of the fluid species with the aerosol dynamics is required to be modeled if the aerosol processes are limited by the ~~concentrations of the gases~~ vapor concentrations, not by time.

Conversely, the Eulerian model can produce more detailed spatial information compared to the Lagrangian model, and the diffusion is also included in simulations. However, it is computationally more expensive; and therefore, the spatial resolution may remain too low to be able to produce realistic results, if the same computational effort as for the Lagrangian model is considered.

4.3 Dependence of volatile nucleation mode concentration on sulfuric acid vapor concentration

It can be seen from Fig. 16 that the nucleation exponent $n_{sa} = 0.25$ fits better for R cases and the nucleation exponent $n_{sa} = 1$ better for A cases. The nucleation exponent 0.25 could also fit to A cases equally well in the sulfuric acid vapor concentration range between 2×10^{10} and $3 \times 10^{11} \text{ cm}^{-3}$. For R cases, there is also one measurement point with the lowest vapor concentration that fits well with the nucleation exponent 1.

However, ~~there could have been underestimated particle concentrations with the lowest sulfuric acid concentrations~~ particle concentrations in A cases ~~because the particle sizes were very low (~ 4 nm) may have been underestimated because of very low particle sizes (CMD ≈ 4 nm), for which detection efficiency~~ for particle measurement devices ~~That underestimation was modeled by calculating the particles larger than 3.6 nm only (green lines in Fig. 16), which is the cut-size D_{50} of used is low. The effect of the detection efficiency was tested by multiplying the modeled particle distributions by the detection efficiency curve for the particle counter TSI CPC 3025, according to Mordas et al. (2008) used in the measurements. The detection efficiency curve is defined by Mordas et al. (2008) for the same CPC model, but for silver particles. The calculated detected particle number concentration is shown in Fig. 16 with gray lines. This decreased the particle concentrations and increased the slope of slopes of the particle concentration very slightly, which is compared to the modeled total particle concentrations. The increase of the slopes is~~

obviously not enough for the nucleation exponent 0.25 to fit in all A cases. However, ~~measured detailed~~ particle size data from A ~~cases measurements~~ are not available, but they range between 4 and 5.5 nm (Arnold et al., 2012). Additionally, particle losses inside the particle measurement setup and devices increase with decreasing particle size; ~~thus the measured particle concentrations can then be underestimated even more, which can affect the slopes also.~~

The nucleation exponent n_{sa} can be estimated directly from the measurement data through the slope of N_{vol} vs. $[H_2SO_4]$, which are also 0.25 and 1. It is not always possible to estimate the nucleation exponent in this manner; because particle number concentration is not only dependent on nucleation rate, but on other aerosol processes too. Condensation and coagulation sinks have effects on the number concentration, especially for the case where soot particles exist, due to increased sinks. In these cases, the sinks resulting from solid particles were not sufficient to cause the slope to differ from the nucleation exponent, although about 77 % of sulfuric acid vapor was condensed onto the solid particles. The effect of the sinks can be seen by comparing the particle number concentration levels in Fig. 16, where R cases have lower values compared to A cases. However, the soot particle sinks ~~can may~~ be underestimated, because soot particles were modeled as spherical particles; which have different ~~particle surface area surface areas~~ compared to fractal particles.

For ~~these our~~ cases, the nucleation exponents n_{sa} between 0.25 and 1 seem to produce the best results. Due to low nucleation exponents, especially when they are below unity when the nucleated cluster would have less than one sulfuric acid molecule according to the first nucleation theorem, it is probable that there are other compounds; ~~such as low-volatile hydrocarbons, that account accounting~~ in the nucleation process. Such other compounds could be, e.g., low-volatile hydrocarbon vapors because they are also found in the particles. More realistic nucleation exponents may be obtained if a separate nucleation mechanism

for hydrocarbon nucleation is modeled, e.g., type of

$$J = K_1[\text{H}_2\text{SO}_4]^2 + K_2[\text{H}_2\text{SO}_4][\text{org}], \quad (14)$$

where [org] is some organics accounting in nucleation, has provided the most reliable results compared to BHN, activation, or kinetic nucleation (Pirjola et al., 2015). [Highly oxidized biogenic organic vapors are also found to have an effect on nucleation rate in atmospheric research of Riccobono et al. \(2014\)](#). Validating attempts to model organic nucleation in vehicle exhaust would need both sulfuric acid vapor and comprehensive hydrocarbon measurements in raw exhaust with particle distribution measurements.

The reason for different nucleation exponents between A and R cases is not obvious, and further research is required to examine that. The difference could be accounted for by different sulfuric acid concentration range vapor concentration ranges, different particle size ranges, or another reason that cannot be seen from the measurements or the simulations studied here. Sulfuric acid vapor concentration range could cause the difference if the nucleation exponent were dependent on the sulfuric acid vapor concentration in a way that the nucleation exponent decreases with increasing sulfuric acid vapor concentration, which is actually seen in CNT. Different particle size range could explain the difference due to decreased counting efficiency with decreasing particle size; particle sizes were lower in A cases compared to R cases.

5 Conclusions

The CFD-TUTEAM model was used to simulate the particle formation process in the a laboratory-scale diesel exhaust sampling system. A, consisting of a porous tube type diluter and an aging chamber were modeled as the sampling system. Eulerian and Lagrangian type . Eulerian- and Lagrangian-type sub-models were used, and the both models produced almost the same particle distributions at the outlet of the aging chamber, but it was seen that the Lagrangian model may not produce realistic results in the inner areas of the sampling

system. The Lagrangian model is computationally less expensive compared to the Eulerian model; thus, it can be modeled with a ~~very high temporal resolution~~ higher temporal resolution with the same computational cost. However, cooling and dilution profiles from the Eulerian model are required as inputs for the Lagrangian model. Conversely, the Eulerian model produced more detailed spatial information inside the sampling system, and it includes diffusion modeling. The main advantage of the modal aerosol model is that it can be used to examine particle formation spatially with lower computational cost compared to sectional aerosol models. The drawback of it relates to the assumption that the particle distributions remain log-normal, which is not true especially when nucleation and condensation occur simultaneously.

The highest nucleation rates were found to exist in the region where hot exhaust and cold dilution air encounter. However, due to low dilution ratio and low nucleation exponents, the nucleation rate remains high in the aging chamber, where the dilution process is already finished. Hence, the major part (over 99 %) of the volatile nucleation mode particles was formed in the aging chamber. With a higher nucleation exponent, the nucleation rate would diminish more steeply in the dilution region; thus, the major part of nucleation would occur in the diluter. Additional experimental data for examining the nucleation exponent could be obtained by measuring particle concentrations inside the aging chamber or with aging chambers of different lengths. If nucleation exponents are low in reality, the major part of nucleation will occur in the aging chamber; therefore, it is not obvious that the nucleation process will be ~~stopped~~ quenched inside the secondary dilution.

The nucleation exponents for sulfuric acid vapor in the range from 0.25 to 1 appeared to fit best with the measurement data, according to the simulations. In this range of condensation and coagulation sinks resulting from solid particles, the nucleation exponents can be estimated directly from the measurement data through the slope of the volatile nucleation mode number concentration vs. the raw exhaust sulfuric acid vapor concentration. Due to the nucleation exponents below unity, it is probable that there are other compounds, such as organics, ~~which affect on~~ affecting the nucleation rate. The reason for different nucleation

exponents between the cases is not obvious, and further research is required to examine that.

According to the simulations, the major part of deposition occurs in the region of the expander of the aging chamber. Turbulence increases in the expander, which increases the effective diffusion coefficient; and therefore, deposition rate increases. The expander had higher influence on the core and soot mode compared to the volatile nucleation mode, because the major part of the volatile nucleation mode particles was formed after the expander.

Appendix A: Detailed description of condensation modeling

A1 Mass growth rate equation

Modeled particle diameters are in the range from a molecule diameter to below 1 μm . This range participates in free-molecular, transition, and continuum regions. The Fuchs–Sutugin correction factor β_i (Seinfeld and Pandis, 2006) in the growth rate equation allows smooth behavior of condensation in all the regions. Especially for hydrocarbons, the growth rate calculation requires the molecule diameter d_i with very small particles, which is included in the equation as $(d_p + d_i)$ (Lehtinen and Kulmala, 2003).

The mass growth rate of a single particle in mode j by a condensing gas-vapor i becomes

$$\frac{\partial m_{p,j,i}}{\partial t} = \frac{2\pi m_i}{k_B T} (d_p + d_i) \beta_i (D_{p,\text{lam}} + D_{i,\text{lam}}) (p_i - p_{i,p}), \quad (\text{A1})$$

where m_i , $D_{i,\text{lam}}$, p_i , and $p_{i,p}$ are the molecule mass, diffusion coefficient, partial pressure, and vapor pressure on the particle surface of a gas-vapor i , respectively. For water and

sulfuric acid vapors, $p_{i,p}$ is calculated by

$$p_{i,p} = \frac{A_{sa-w}}{A_p} \Gamma_i K_i p_i^\circ, \quad (A2)$$

where A_{sa-w} is the surface area of sa-w phase in a particle, and A_p is the surface area of the whole particle. Γ_i , K_i , p_i° are activity (Taleb et al., 1996), Kelvin factor, and saturation vapor pressure of gas-vapor i . For hydrocarbonshydrocarbon vapors, the last term of Eq. (A1) is computed as

$$(p_i - p_{i,p}) = f_{hc} p_{hc}. \quad (A3)$$

Kelvin factor for water and sulfuric acid is calculated by

$$K_i = \exp\left(\frac{4\sigma_{sa-w}m_i}{k_B T \rho_{sa-w}d_p}\right), \quad (A4)$$

where σ_{sa-w} and ρ_{sa-w} are surface tension (Vehkamäki et al., 2003) and density (Vehkamäki et al., 2002) of sa-w solution.

A2 Phase interactions

Liquid parts in particles are considered two immiscible phases: sulfuric acid-water phase (sa-w) and hydrocarbon (hc) phase. The phase with lower volume fraction is assumed to form a lens on the surface of the hydrocarbon-other phase (Ziemann and McMurry, 1998) as shown in Fig. 2. The surface area of the whole particle A_p is considered the area onto which condensation occurs, regardless of the particle composition. However e.g., sulfuric acid does not evaporate from a particle from the area of hc phase. Therefore, the fraction $\frac{A_{sa-w}}{A_p}$ is used in Eq. (A2). The fraction can be obtained from geometrical calculations, and

the following fitting functions are used as-for it:

$$\frac{A_{\text{minor}}}{A_p} = 0.237 \left(\frac{V_{\text{minor}}}{V_p} \right) + 0.539 \left(\frac{V_{\text{minor}}}{V_p} \right)^{\frac{1}{2}} \quad (\text{A5})$$

for the volatile nucleation mode. Subscript minor presents the phase with the minority of the volume V in the particle. For the core mode, the fraction is

$$\frac{A_{\text{minor}}}{A_p} = 0.237 \left[\frac{V_{\text{minor}}}{V_p} (1 - d'^3) \right] + 0.539 \left[\frac{V_{\text{minor}}}{V_p} (1 - d'^3) \right]^{\frac{1}{2}} \quad (\text{A6})$$

if

$$\frac{V_{\text{minor}}}{V_p} < \frac{(1 - d')^2 (2 + d')}{4(1 - d'^3)} \quad (\text{A7})$$

and

$$\frac{A_{\text{minor}}}{A_p} = (0.336d'^{1.602} + 0.667) \left(\frac{V_{\text{minor}}}{V_p} \right) - 0.168d'^{1.602} + 0.167 \quad (\text{A8})$$

otherwise. In the equation, $d' = \frac{d_{\text{core}}}{d_p}$, where d_{core} denotes the solid core diameter in the non-volatile nucleation mode particle. Due to more complex geometry of soot particles, a constant value of unity, as an approximation, for the fraction is used for the soot mode.

A3 Fraction of condensing hydrocarbons

Due to a wide range of different hydrocarbons in diesel exhaust, it is not reasonable to model them all. A new method to model hydrocarbons is implemented in the model. According to Donahue et al. (2006), hydrocarbons in diesel exhaust can be partitioned to bins with different volatilities. Hydrocarbons with partial pressure over higher than corresponding vapor pressure on the particle are considered the fraction that is able to condense onto

~~the particle phase~~ condensing hydrocarbon vapor fraction. These hydrocarbons satisfy the equation

$$p_{\text{hc}} > \frac{A_{\text{hc}}}{A_{\text{p}}} \Gamma_{\text{hc}} p_{\text{hc}}^{\circ}(T), \quad (\text{A9})$$

where Kelvin factor calculation is neglected due to a wide range of the properties of different hydrocarbons. Unity is used as a value for activity of hydrocarbons Γ_{hc} .

Assuming the diesel exhaust organic aerosol volatility distribution measured by May et al. (2013), with a temperature T in Kelvins and partial pressure of total hydrocarbons p_{hc} in Pascals, the mass fraction of

$$f_{\text{hc}}(p_{\text{hc}}, T) = \left[1 + p_{\text{hc}}^{-0.7} \exp\left(-\frac{5457}{T} + 11.83\right) \right]^{-1} \quad (\text{A10})$$

of hydrocarbons satisfy Eq. (A9). The volatility distribution is measured from the aerosol phase, but it is used here as the volatility distribution of the gas phase, due to the lack of ~~such distribution~~ such a distribution. The side of the lowest volatilities of the distribution is, however, approximately equal for the gas phase distribution too (Donahue et al., 2006). Therefore, Eq. (A10) is valid only when $f_{\text{hc}} \lesssim 0.5$. In ~~these cases~~ this study, f_{hc} is always below 0.4. Modeled hydrocarbons exclude volatile organic compounds ~~;~~ because they are not present in the aerosol phase volatility distribution. However, during the condensation process, the hydrocarbon distribution is changed due to the assumption that condensation consumes ~~hydrocarbons~~ hydrocarbon vapors with the highest saturation ratios first. Therefore, the fraction of condensable ~~hydrocarbons~~ hydrocarbon vapors is decreasing during the condensation process. This is included in the model by subtracting the fraction of already condensed ~~hydrocarbons~~ hydrocarbon vapors, $f_{\text{hc,cond}}$ from Eq. (A10), and it is defined as

$$f_{\text{hc,cond}} = \frac{\sum_j M_{j,1,\text{hc}}}{\sum_j M_{j,1,\text{hc}} + C_{\text{hc}}}, \quad (\text{A11})$$

where C_{hc} is the mass concentration of hydrocarbon mixture remaining in the gas phase.

The properties of tetracosane ($C_{24}H_{50}$) are used as the properties of hydrocarbon mixture $\bar{\gamma}$ because 24 is the average carbon chain length ~~in alkanes of the~~ of the alkanes in the diesel exhaust particles, according to Schauer et al. (1999). The mass fraction of condensable ~~hydrocarbons~~ hydrocarbon vapors is used instead of the mole fraction $\bar{\gamma}$ because the hydrocarbon mixture is modeled as the average carbon chain and the condensation rate is modeled as mass basis.

A4 Water equilibrium computation procedure

A particle in water equilibrium is defined as a particle onto which no condensation and from which no evaporation of water vapor occurs. Therefore, the following equation is satisfied:

$$RH = \frac{A_{sa-w}}{A_p}(T, \mathbf{Y}^{eq}) \Gamma_w(T, \mathbf{Y}^{eq}) K_w(T, \mathbf{Y}^{eq}, d_p), \quad (A12)$$

where \mathbf{Y}^{eq} denotes the particle composition in water equilibrium.

The factor for water equilibrium κ_j in Eq. (8) is altered after every iteration of CFD software until the volatile and nonvolatile nucleation mode particles in the whole computational domain are in water equilibrium. Ensuring water equilibrium is performed by checking that the particles satisfy Eq. (A12). Initially $\kappa_j = 1$, ~~thus;~~ thus, the composition \mathbf{Y}^{eq} solved from Eq. (A12) is ~~used to obtain as~~ an initial guess for the iterative procedure of water equilibrium.

For the Lagrangian model, water equilibrium is maintained by altering water content in the particles artificially after every time step in a way such a manner that Eq. (A12) is satisfied.

Acknowledgements. This work was funded by the Maj and Tor Nessling foundation (project number 2014452), by the Finnish Funding Agency for Technology and Innovation, Tekes (TREAM project), and by Dinex Ecocat Oy, Neste Oil Oyj, AGCO Power, and Ab Nanol Technologies Oy.

References

- Albriet, B., Sartelet, K., Lacour, S., Carissimo, B., and Seigneur, C.: Modelling aerosol number distributions from a vehicle exhaust with an aerosol CFD model, *Atmos. Environ.*, 44, 1126–1137, doi:10.1016/j.atmosenv.2009.11.025, 2010.
- Alföldy, B., Giechaskiel, B., Hofmann, W., and Drossinos, Y.: Size-distribution dependent lung deposition of diesel exhaust particles, *J. Aerosol Sci.*, 40, 652–663, doi:10.1016/j.jaerosci.2009.04.009, 2009.
- Allen, M. and Raabe, O.: Slip correction measurements of spherical solid aerosol particles in an improved Millikan apparatus, *Aerosol Sci. Tech.*, 4, 269–286, doi:10.1080/02786828508959055, 1985.
- ANSYS: ANSYS FLUENT 14.0 software manual, Canonsburg, USA, 2011.
- Arnth, A., Unger, N., Kulmala, M., and Andreae, M.: Clean the air, heat the planet?, *Science*, 326, 672–673, doi:10.1126/science.1181568, 2009.
- Arnold, F., Pirjola, L., Rönkkö, T., Reichl, U., Schlager, H., Lähde, T., Heikkilä, J., and Keskinen, J.: First online measurements of sulfuric acid gas in modern heavy-duty diesel engine exhaust: implications for nanoparticle formation, *Environ. Sci. Technol.*, 46, 11227–11234, doi:10.1021/es302432s, 2012.
- Beelen, R., Raaschou-Nielsen, O., Stafoggia, M., Andersen, Z., Weinmayr, G., Hoffmann, B., Wolf, K., Samoli, E., Fischer, P., Nieuwenhuijsen, M., Vineis, P., Xun, W., Katsouyanni, K., Dimakopoulou, K., Oudin, A., Forsberg, B., Modig, L., Havulinna, A., Lanki, T., Turunen, A., Oftedal, B., Nystad, W., Nafstad, P., De Faire, U., Pedersen, N., Östenson, C.-G., Fratiglioni, L., Penell, J., Korek, M., Pershagen, G., Eriksen, K., Overvad, K., Ellermann, T., Eeftens, M., Peeters, P., Meliefste, K., Wang, M., Bueno-De-Mesquita, B., Sugiri, D., Krämer, U., Heinrich, J., De Hoogh, K., Key, T., Peters, A., Hampel, R., Concin, H., Nagel, G., Ineichen, A., Schaffner, E., Probst-Hensch, N., Künzli, N., Schindler, C., Schikowski, T., Adam, M., Phuleria, H., Vilier, A., Clavel-Chapelon, F., Declercq, C., Grioni, S., Krogh, V., Tsai, M.-Y., Ricceri, F., Sacerdote, C., Galassi, C., Migliore, E., Ranzi, A., Cesaroni, G., Badaloni, C., Forastiere, F., Tamayo, I., Amiano, P., Dorronsoro, M., Katsoulis, M., Trichopoulou, A., Brunekreef, B., and Hoek, G.: Effects of long-term exposure to air pollution on natural-cause mortality: an analysis of 22 European cohorts within the multicentre ESCAPE project, *Lancet*, 383, 785–795, doi:10.1016/S0140-6736(13)62158-3, 2014.

- Dockery, D., Pope III, C., Xu, X., Spengler, J., Ware, J., Fay, M., Ferris Jr., B., and Speizer, F.: An association between air pollution and mortality in six U.S. cities, *New Engl. J. Med.*, 329, 1753–1759, doi:10.1056/NEJM199312093292401, 1993.
- Donahue, N. M., Robinson, A. L., Stanier, C. O., and Pandis, S. N.: Coupled partitioning, dilution, and chemical aging of semivolatile organics, *Environ. Sci. Technol.*, 40, 2635–2643, doi:10.1021/es052297c, 2006.
- Giechaskiel, B., Ntziachristos, L., and Samaras, Z.: Effect of ejector dilutors on measurements of automotive exhaust gas aerosol size distributions, *Meas. Sci. Technol.*, 20, 045703, doi:10.1088/0957-0233/20/4/045703, 2009.
- [Herrmann, E., Ding, A. J., Kerminen, V.-M., Petäjä, T., Yang, X. Q., Sun, J. N., Qi, X. M., Manninen, H., Hakala, J., Nieminen, T., Aalto, P. P., Kulmala, M., and Fu, C. B.: Aerosols and nucleation in eastern China: first insights from the new SORPES-NJU station, *Atmos. Chem. Phys.*, 14, 2169–2183, doi:10.5194/acp-14-2169-2014, 2014.](#)
- Hinds, W. C.: *Aerosol Technology: Properties, Behavior, and Measurement of Airborne Particles*, 2nd edn., John Wiley and Sons, Inc., Hoboken, USA, 1999.
- Huang, L., Gong, S. L., Gordon, M., Liggio, J., Staebler, R., Stroud, C. A., Lu, G., Mihele, C., Brook, J. R., and Jia, C. Q.: Aerosol–computational fluid dynamics modeling of ultrafine and black carbon particle emission, dilution, and growth near roadways, *Atmos. Chem. Phys.*, 14, 12631–12648, doi:10.5194/acp-14-12631-2014, 2014.
- [Iland, K., Wedekind, J., Wölk, J., Wagner, P. E., and Strey, R.: Homogeneous nucleation rates of 1-pentanol, *J. Chem. Phys.*, 121, 12259–12264, doi:10.1063/1.1809115, 2004.](#)
- Johansson, C., Norman, M., and Gidhagen, L.: Spatial and temporal variations of PM₁₀ and particle number concentrations in urban air, *Environ. Monit. Assess.*, 127, 477–487, doi:10.1007/s10661-006-9296-4, 2007.
- Kashchiev, D.: On the relation between nucleation work, nucleus size, and nucleation rate, *J. Chem. Phys.*, 76, 5098–5102, doi:10.1063/1.442808, 1982.
- Keskinen, J. and Rönkkö, T.: Can real-world diesel exhaust particle size distribution be reproduced in the laboratory? A critical review, *J. Air Waste Manage.*, 60, 1245–1255, doi:10.3155/1047-3289.60.10.1245, 2010.
- Kittelson, D.: Engines and nanoparticles: a review, *J. Aerosol Sci.*, 29, 575–588, doi:10.1016/S0021-8502(97)10037-4, 1998.
- Kittelson, D., Watts, W., Johnson, J., Thorne, C., Higham, C., Payne, M., Goodier, S., Warrens, C., Preston, H., Zink, U., Pickles, D., Goersmann, C., Twigg, M., Walker, A., and Boddy, R.: Effect of

- fuel and lube oil sulfur on the performance of a diesel exhaust gas continuously regenerating trap, *Environ. Sci. Technol.*, 42, 9276–9282, doi:10.1021/es703270j, 2008.
- Kulmala, M. and Laaksonen, A.: Binary nucleation of water-sulfuric acid system: Comparison of classical theories with different H_2SO_4 saturation vapor pressures, *J. Chem. Phys.*, 93, 696–701, doi:10.1063/1.459519, 1990.
- Kulmala, M., Lehtinen, K. E. J., and Laaksonen, A.: Cluster activation theory as an explanation of the linear dependence between formation rate of 3nm particles and sulphuric acid concentration, *Atmos. Chem. Phys.*, 6, 787–793, doi:10.5194/acp-6-787-2006, 2006.
- Kulmala, M., Riipinen, I., Sipilä, M., Manninen, H. E., Petäjä, T., Junninen, H., Dal Maso, M., Moradas, G., Mirme, A., Vana, M., Hirsikko, A., Laakso, L., Harrison, R. M., Hanson, I., Leung, C., Lehtinen, K. E. J., and Kerminen, V.-M.: Toward direct measurement of atmospheric nucleation, *Science*, 318, 89–92, doi:10.1126/science.1144124, 2007.
- Kupiainen-Määttä, O., Olenius, T., Korhonen, H., Malila, J., Dal Maso, M., Lehtinen, K., and Vehkamäki, H.: Critical cluster size cannot in practice be determined by slope analysis in atmospherically relevant applications, *J. Aerosol Sci.*, 77, 127–144, doi:10.1016/j.jaerosci.2014.07.005, 2014.
- Lehtinen, K. E. J. and Kulmala, M.: A model for particle formation and growth in the atmosphere with molecular resolution in size, *Atmos. Chem. Phys.*, 3, 251–257, doi:10.5194/acp-3-251-2003, 2003.
- Lemmetty, M., Pirjola, L., Mäkelä, J., Rönkkö, T., and Keskinen, J.: Computation of maximum rate of water-sulphuric acid nucleation in diesel exhaust, *J. Aerosol Sci.*, 37, 1596–1604, doi:10.1016/j.jaerosci.2006.04.003, 2006.
- Lemmetty, M., Rönkkö, T., Virtanen, A., Keskinen, J., and Pirjola, L.: The effect of sulphur in diesel exhaust aerosol: models compared with measurements, *Aerosol Sci. Tech.*, 42, 916–929, doi:10.1080/02786820802360682, 2008.
- Li, X. and Huang, Z.: Formation and transformation of volatile nanoparticles from a diesel engine during exhaust dilution, *Chinese Sci. Bull.*, 57, doi:10.1007/s11434-011-4927-8, 2012.
- Liu, Y. H., He, Z., and Chan, T. L.: Three-dimensional simulation of exhaust particle dispersion and concentration fields in the near-wake region of the studied ground vehicle, *Aerosol Sci. Tech.*, 45, 1019–1030, doi:10.1080/02786826.2011.580021, 2011.
- Lyyräinen, J., Jokiniemi, J., Kauppinen, E. I., Backman, U., and Vesala, H.: Comparison of different dilution methods for measuring diesel particle emissions, *Aerosol Sci. Tech.*, 38, 12–23, doi:10.1080/02786820490247579, 2004.

- Maricq, M., Chase, R., Xu, N., and Laing, P.: The effects of the catalytic converter and fuel sulfur level on motor vehicle particulate matter emissions: light duty diesel vehicles, *Environ. Sci. Technol.*, 36, 283–289, doi:10.1021/es010962l, 2002.
- Mathis, U., Mohr, M., and Zenobi, R.: Effect of organic compounds on nanoparticle formation in diluted diesel exhaust, *Atmos. Chem. Phys.*, 4, 609–620, doi:10.5194/acp-4-609-2004, 2004a.
- Mathis, U., Ristimäki, J., Mohr, M., Keskinen, J., Ntziachristos, L., Samaras, Z., and Mikkanen, P.: Sampling conditions for the measurement of nucleation mode particles in the exhaust of a diesel vehicle, *Aerosol Sci. Tech.*, 38, 1149–1160, doi:10.1080/027868290891497, 2004b.
- May, A. A., Presto, A. A., Hennigan, C. J., Nguyen, N. T., Gordon, T. D., and Robinson, A. L.: Gas-particle partitioning of primary organic aerosol emissions: (2) Diesel vehicles, *Environ. Sci. Technol.*, 47, 8288–8296, doi:10.1021/es400782j, 2013.
- McMurry, P. and Friedlander, S.: New particle formation in the presence of an aerosol, *Atmos. Environ.*, 13, 1635–1651, doi:10.1016/0004-6981(79)90322-6, 1979.
- Mordas, G., Manninen, H., Petäjä, T., Aalto, P., Hämeri, K., and Kulmala, M.: On operation of the ultra-fine water-based CPC TSI 3786 and comparison with other TSI models (TSI 3776, TSI 3772, TSI 3025, TSI 3010, TSI 3007), *Aerosol Sci. Tech.*, 42, 152–158, doi:10.1080/02786820701846252, 2008.
- Ntziachristos, L., Giechaskiel, B., Pistikopoulos, P., Samaras, Z., Mathis, U., Mohr, M., Ristimäki, J., Keskinen, J., Mikkanen, P., Casati, R., Scheer, V., and Vogt, R.: Performance evaluation of a novel sampling and measurement system for exhaust particle characterization, *SAE Tech. Paper Ser.*, 2004-01-1439, doi:10.4271/2004-01-1439, 2004.
- Olin, M., Dal Maso, M., and Rönkkö, T.: Sulfur driven nucleation in diesel exhaust: simulations of a laboratory sampling system, in: *Proceedings of the 18th ETH-Conference on Combustion Generated Nanoparticles*, Zürich, Switzerland, 22–25 June 2014, 45–46, 2014.
- Paasonen, P., Nieminen, T., Asmi, E., Manninen, H. E., Petäjä, T., Plass-Dülmer, C., Flentje, H., Birmili, W., Wiedensohler, A., Hörrak, U., Metzger, A., Hamed, A., Laaksonen, A., Facchini, M. C., Kerminen, V.-M., and Kulmala, M.: On the roles of sulphuric acid and low-volatility organic vapours in the initial steps of atmospheric new particle formation, *Atmos. Chem. Phys.*, 10, 11223–11242, doi:10.5194/acp-10-11223-2010, 2010.
- Pey, J., Querol, X., Alastuey, A., Rodriguez, S., Putaud, J., and Van Dingenen, R.: Source apportionment of urban fine and ultra-fine particle number concentration in a Western Mediterranean city, *Atmos. Environ.*, 43, 4407–4415, doi:10.1016/j.atmosenv.2009.05.024, 2009.

- Pirjola, L., Karl, M., Rönkkö, T., and Arnold, F.: Model studies ~~on the formation~~ of volatile diesel exhaust ~~particles: are~~ particle formation: organic vapours involved in nucleation and growth?, ~~submitted to~~ Atmos. Chem. Phys. Discuss., 2014–15, 4219–4263, doi:10.5194/acpd-15-4219-2015, 2015.
- Pope, C., Burnett, R., Thun, M., Calle, E., Krewski, D., Ito, K., and Thurston, G.: Lung cancer, cardiopulmonary mortality, and long-term exposure to fine particulate air pollution, J. Amer. Med. Assoc., 287, 1132–1141, doi:10.1001/jama.287.9.1132, 2002.
- Pyykönen, J., Miettinen, M., Sippula, O., Leskinen, A., Raunemaa, T., and Jokiniemi, J.: Nucleation in a perforated tube diluter, J. Aerosol Sci., 38, 172–191, doi:10.1016/j.jaerosci.2006.11.006, 2007.
- Riccobono, F., Schobesberger, S., Scott, C. E., Dommen, J., Ortega, I. K., Rondo, L., Almeida, J., Amorim, A., Bianchi, F., Breitenlechner, M., David, A., Downard, A., Dunne, E. M., Duplissy, J., Ehrhart, S., Flagan, R. C., Franchin, A., Hansel, A., Junninen, H., Kajos, M., Keskinen, H., Kupc, A., Kürten, A., Kvashin, A. N., Laaksonen, A., Lehtipalo, K., Makhmutov, V., Mathot, S., Nieminen, T., Onnela, A., Petäjä, T., Praplan, A. P., Santos, F. D., Schallhart, S., Seinfeld, J. H., Sipilä, M., Spracklen, D. V., Stozhkov, Y., Stratmann, F., Tomé, A., Tsagkogeorgas, G., Vaattovaara, P., Viisanen, Y., Virtala, A., Wagner, P. E., Weingartner, E., Wex, H., Wimmer, D., Carslaw, K. S., Curtius, J., Donahue, N. M., Kirkby, J., Kulmala, M., Worsnop, D. R., and Baltensperger, U.: Oxidation Products of Biogenic Emissions Contribute to Nucleation of Atmospheric Particles, Science, 344, 717–721, doi:10.1126/science.1243527, 2014.
- Rissler, J., Swietlicki, E., Bengtsson, A., Boman, C., Pagels, J., Sandström, T., Blomberg, A., and Löndahl, J.: Experimental determination of deposition of diesel exhaust particles in the human respiratory tract, J. Aerosol Sci., 48, 18–33, doi:10.1016/j.jaerosci.2012.01.005, 2012.
- Rönkkö, T., Virtanen, A., Vaaraslahti, K., Keskinen, J., Pirjola, L., and Lappi, M.: Effect of dilution conditions and driving parameters on nucleation mode particles in diesel exhaust: laboratory and on-road study, Atmos. Environ., 40, 2893–2901, doi:10.1016/j.atmosenv.2006.01.002, 2006.
- Rönkkö, T., Virtanen, A., Kannosto, J., Keskinen, J., Lappi, M., and Pirjola, L.: Nucleation mode particles with a nonvolatile core in the exhaust of a heavy duty diesel vehicle, Environ. Sci. Technol., 41, 6384–6389, doi:10.1021/es0705339, 2007.
- Rönkkö, T., Lähde, T., Heikkilä, J., Pirjola, L., Bauschke, U., Arnold, F., Schlager, H., Rothe, D., Yli-Ojanperä, J., and Keskinen, J.: Effects of gaseous sulphuric acid on diesel exhaust nanoparticle formation and characteristics, Environ. Sci. Technol., 47, 11882–11889, doi:10.1021/es402354y, 2013.

- Sakurai, H., Tobias, H., Park, K., Zarling, D., Docherty, K., Kittelson, D., McMurry, P., and Ziemann, P.: On-line measurements of diesel nanoparticle composition and volatility, *Atmos. Environ.*, 37, 1199–1210, doi:10.1016/S1352-2310(02)01017-8, 2003.
- Schauer, J., Kleeman, M., Cass, G., and Simoneit, B.: Measurement of emissions from air pollution sources. 2. C1 through C30 organic compounds from medium duty diesel trucks, *Environ. Sci. Technol.*, 33, 1578–1587, doi:10.1021/es980081n, 1999.
- Schneider, J., Hock, N., Weimer, S., Borrmann, S., Kirchner, U., Vogt, R., and Scheer, V.: Nucleation particles in diesel exhaust: composition inferred from in situ mass spectrometric analysis, *Environ. Sci. Technol.*, 39, 6153–6161, doi:10.1021/es049427m, 2005.
- Seinfeld, J. and Pandis, S.: *Atmospheric Chemistry and Physics: From Air Pollution to Climate Change*, 2nd edn., John Wiley and Sons, Inc., Hoboken, USA, 2006.
- Sgro, L., Borghese, A., Speranza, L., Barone, A., Minutolo, P., Bruno, A., D'Anna, A., and D'Alessio, A.: Measurements of nanoparticles of organic carbon and soot in flames and vehicle exhausts, *Environ. Sci. Technol.*, 42, 859–863, doi:10.1021/es070485s, 2008.
- Sihto, S.-L., Vuollekoski, H., Leppä, J., Riipinen, I., Kerminen, V.-M., Korhonen, H., Lehtinen, K. E. J., Boy, M., and Kulmala, M.: Aerosol dynamics simulations on the connection of sulphuric acid and new particle formation, *Atmos. Chem. Phys.*, 9, 2933–2947, doi:10.5194/acp-9-2933-2009, 2009.
- Taleb, D.-E., Ponche, J.-L., and Mirabel, P.: Vapor pressures in the ternary system water-nitric acid-sulfuric acid at low temperature: a reexamination, *J. Geophys. Res.-Atmos.*, 101, 25967–25977, doi:10.1029/96JD02330, 1996.
- Tobias, H., Beving, D., Ziemann, P., Sakurai, H., Zuk, M., McMurry, P., Zarling, D., Waytulonis, R., and Kittelson, D.: Chemical analysis of diesel engine nanoparticles using a nano-DMA/thermal desorption particle beam mass spectrometer, *Environ. Sci. Technol.*, 35, 2233–2243, doi:10.1021/es0016654, 2001.
- Uhrner, U., von Löwis, S., Vehkamäki, H., Wehner, B., Bräsel, S., Hermann, M., Stratmann, F., Kulmala, M., and Wiedensohler, A.: Dilution and aerosol dynamics within a diesel car exhaust plume-CFD simulations of on-road measurement conditions, *Atmos. Environ.*, 41, 7440–7461, doi:10.1016/j.atmosenv.2007.05.057, 2007.
- Vaaraslahti, K., Keskinen, J., Giechaskiel, B., Solla, A., Murtonen, T., and Vesala, H.: Effect of lubricant on the formation of heavy-duty diesel exhaust nanoparticles, *Environ. Sci. Technol.*, 39, 8497–8504, doi:10.1021/es0505503, 2005.

[Vanhanen, J., Mikkilä, J., Lehtipalo, K., Sipilä, M., Manninen, H. E., Siivola, E., Petäjä, T., and Kulmala, M.: Particle size magnifier for nano-CN detection, *Aerosol Sci. Tech.*, 45, 533–542, doi:10.1080/02786826.2010.547889, 2011.](#)

Vehkamäki, H. and Riipinen, I.: Thermodynamics and kinetics of atmospheric aerosol particle formation and growth, *Chem. Soc. Rev.*, 41, 5160–5173, doi:10.1039/C2CS00002D, 2012.

Vehkamäki, H., Kulmala, M., Napari, I., Lehtinen, K., Timmreck, C., Noppel, M., and Laaksonen, A.: An improved parameterization for sulfuric acid-water nucleation rates for tropospheric and stratospheric conditions, *J. Geophys. Res.-Atmos.*, 107, AAC 3–1–AAC 3–10, doi:10.1029/2002JD002184, 2002.

Vehkamäki, H., Kulmala, M., Lehtinen, K., and Noppel, M.: Modelling binary homogeneous nucleation of water-sulfuric acid vapours: parameterisation for high temperature emissions, *Environ. Sci. Technol.*, 37, 3392–3398, doi:10.1021/es0263442, 2003.

Virtanen, A., Ristimäki, J., Marjamäki, M., Vaaraslahti, K., Keskinen, J., and Lappi, M.: Effective density of diesel exhaust particles as a function of size, *SAE Tech. Paper Ser.*, 2002-01-0056, doi:10.4271/2002-01-0056, 2002.

Virtanen, A., Rönkkö, T., Kannosto, J., Ristimäki, J., Mäkelä, J. M., Keskinen, J., Pakkanen, T., Hillamo, R., Pirjola, L., and Hämeri, K.: Winter and summer time size distributions and densities of traffic-related aerosol particles at a busy highway in Helsinki, *Atmos. Chem. Phys.*, 6, 2411–2421, doi:10.5194/acp-6-2411-2006, 2006.

Vogt, R., Scheer, V., Casati, R., and Benter, T.: On-road measurement of particle emission in the exhaust plume of a diesel passenger car, *Environ. Sci. Technol.*, 37, 4070–4076, doi:10.1021/es0300315, 2003.

Voultzis, E., Ntziachristos, L., and Samaras, Z.: Modelling of diesel exhaust aerosol during laboratory sampling, *Atmos. Environ.*, 39, 1335–1345, doi:10.1016/j.atmosenv.2004.11.011, 2005.

Wang, Y. and Zhang, K.: Coupled turbulence and aerosol dynamics modeling of vehicle exhaust plumes using the CTAG model, *Atmos. Environ.*, 59, 284–293, doi:10.1016/j.atmosenv.2012.04.062, 2012.

[Wang, Z. B., Hu, M., Yue D. L., Zheng, J., Zhang, R. Y., Wiedensohler, A., Wu, Z. J., Nieminen, T., and Boy, M.: Evaluation on the role of sulfuric acid in the mechanisms of new particle formation for Beijing case, *Atmos. Chem. Phys.*, 11, 12663–12671, doi:10.5194/acp-11-12663-2011, 2011.](#)

Whitby, E. and McMurry, P.: Modal aerosol dynamics modeling, *Aerosol Sci. Tech.*, 27, 673–688, doi:10.1080/02786829708965504, 1997.

Wilck, M.: Modal modelling of multicomponent aerosols, Ph. D. thesis, Universität Leipzig, Leipzig, Germany, 1998.

[Wölk, J. and Strey, R.: Homogeneous nucleation of H₂O and D₂O in comparison: the isotope effect, J. Phys. Chem. B, 105, 11683–11701, doi:10.1021/jp0115805, 2001.](#)

Ziemann, P. J. and McMurry, P. H.: Secondary electron yield measurements as a means for probing organic films on aerosol particles, Aerosol Sci. Tech., 28, 77–90, doi:10.1080/02786829808965513, 1998.

Table 1. Boundary conditions for the simulations.

Boundary	Temperature (°C)	sa mole fraction	w mole fraction	hc mole fraction (ppmC ₁)	Flow rate (SLPM)	N_{core} (cm ⁻³)	N_{soot} (cm ⁻³)
Exhaust inlet	~ 430	7×10^{-11} – 4×10^{-8} ^a	0.085	3–8.5 (fitted)	4.5	0 – 5×10^6	0 – 4×10^6
Dilution air inlet	~ 30	0	~ 0.004 (10 % RH)	0	50	0	0
Inner walls	Coupled	Zero flux ^b	0 ^c or zero flux ^b	0 ^c or zero flux ^b	0	0	0

^a Corresponds to 7×10^8 – 4×10^{11} cm⁻³.

^b If saturation ratio is below unity, vapor is not depositing.

^c If saturation ratio is over unity, vapor is depositing.

Table 2. ~~Proportions~~ Modeled proportions of sulfuric acid ~~found~~ existing in different modes and ~~remained~~ remaining in the gas phase (%) at the end of the aging chamber.

Mode	A, $n_{sa} = 1$	R, $n_{sa} = 0.25$
vol	0.5–4	0.2–4
soot	–	72–74
core	–	1.3–4.5
gas	96–99.5	19–22

Table 3. Particle liquid part composition (mass-%) and the maximum saturation vapor pressures of hydrocarbons at the end of the aging chamber.

Mode	A, $n_{sa} = 1$			R, $n_{sa} = 0.25$		
	sa	w	hc	sa	w	hc
vol	2.4–14	0.5–8	77–97	0.6–9.4	0.14–6.2	84–99
soot	–	–	–	0.6–16	0.17–4.7	79–99
core	–	–	–	0.4–11	0.62–7.3	82–99
$p_{hc}^{\circ}(298\text{K})$	$< 5 \times 10^{-7}$ Pa			$< 5 \times 10^{-6}$ – $< 2 \times 10^{-5}$ Pa		

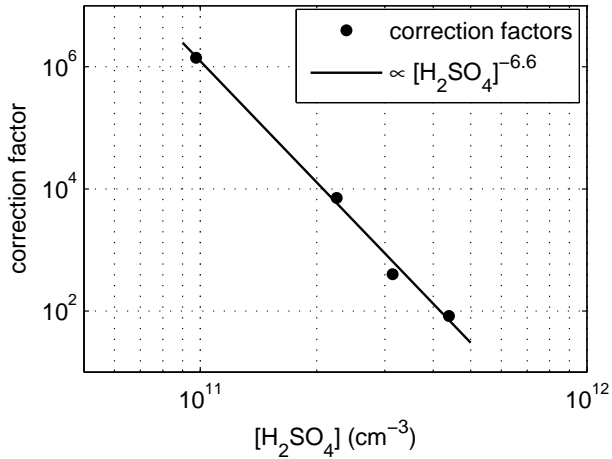


Figure 1. Correction factors for nucleation rate obtained from CNT as a function of raw exhaust sulfuric acid [vapor](#) concentration. Figure adapted from Olin et al. (2014).

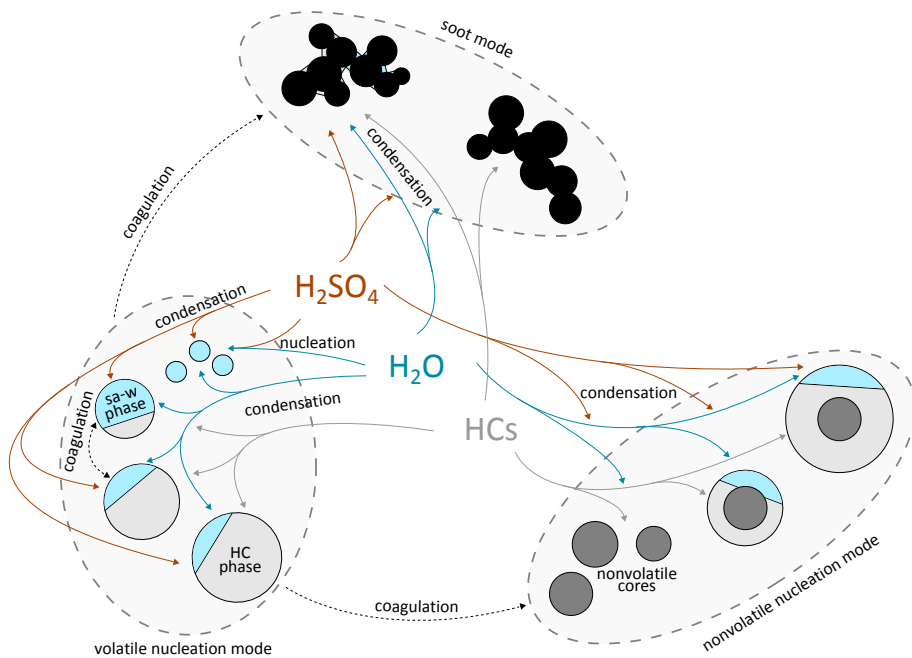


Figure 2. Modeled aerosol processes, modes, components, and phases. Detailed information on them are explained in Sect. 2.2.3 and in Appendix A.

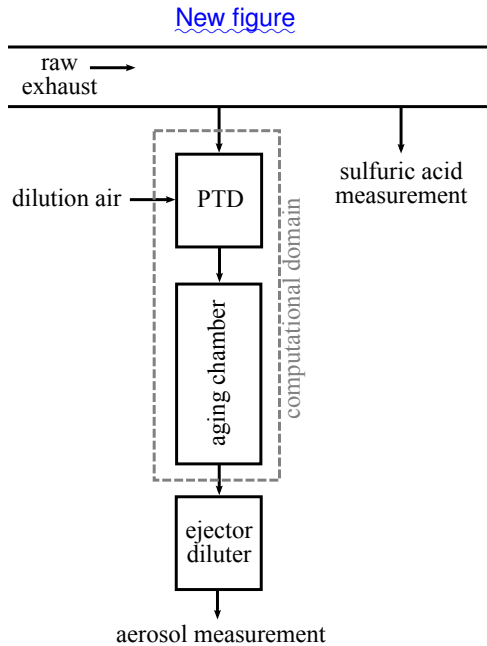


Figure 3. The part of the measurement setup relevant for the simulations. The computational domain consists of a PTD and an aging chamber only due to an approximation that the ejector diluter has a minor effect only on the particle distribution.

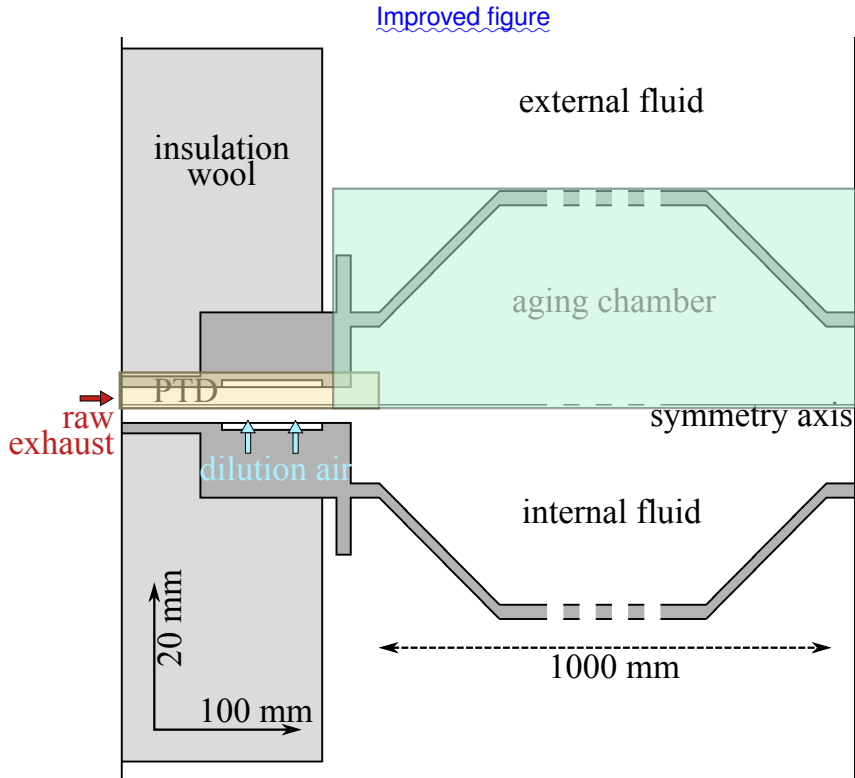


Figure 4. The geometry-computational domain. It is an axial symmetric geometry where the hot raw exhaust inlet is on input from the left, and the dilution air is supplied radially from a cylindrical boundary in the PTD region. The aging chamber continues towards right and it is 1 of length. PTD is insulated but the latter part lies in stagnant external fluid. Only the ends of the aging chamber are shown, but the length of it is 1 m in reality. The figure is scaled vertically with a factor of 5. The yellow (PTD) and the green (aging chamber) boxes present the regions on which the countour plots are plotted in the following figures.

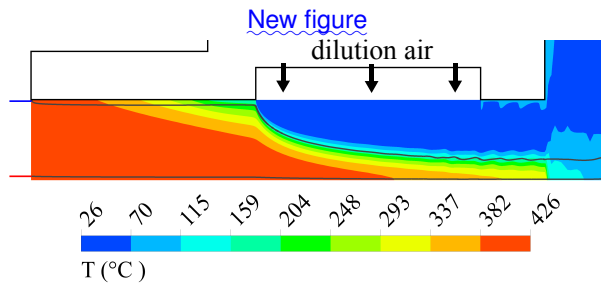


Figure 5. Temperature in the PTD region. The gray lines represent the path lines used in the Lagrangian simulation. Blue and red lines in the beginning of the path lines are the color coding of them. The figure is scaled vertically with a factor of 10.

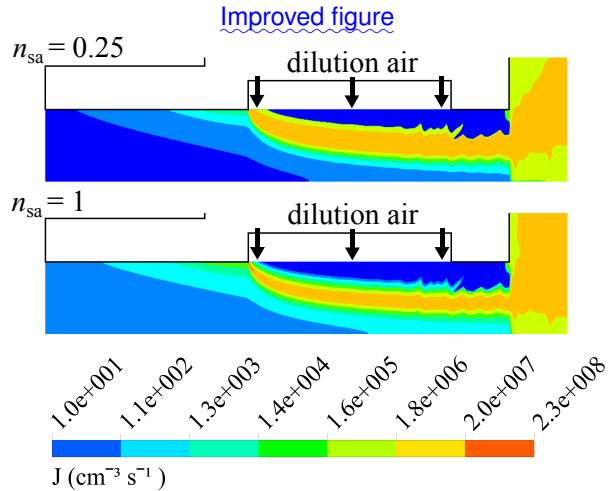


Figure 6. Nucleation rate in the PTD region when there is $[\text{H}_2\text{SO}_4] = 1.47 \times 10^{11} \text{ cm}^{-3}$ in raw exhaust of R case with $n_{sa} = 1$ different nucleation exponents. The figure is scaled vertically with a factor of 10.

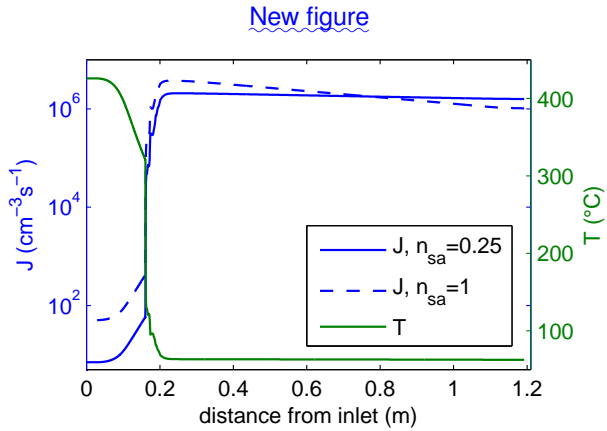


Figure 7. Temperature and nucleation rate at the axis when there is $[H_2SO_4] = 1.47 \times 10^{11} \text{ cm}^{-3}$ in raw exhaust of R case with different nucleation exponents.

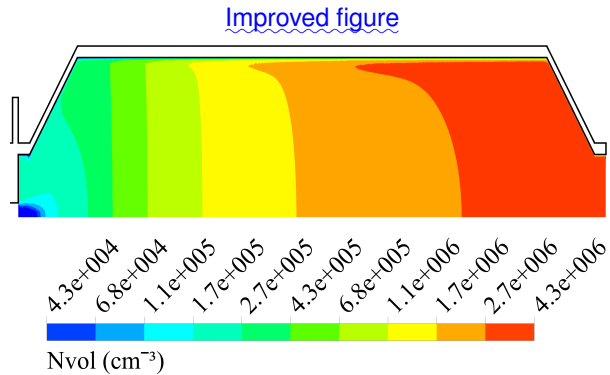


Figure 8. The volatile nucleation mode concentration in the aging chamber region when there is $[\text{H}_2\text{SO}_4] = 1.47 \times 10^{11} \text{ cm}^{-3}$ in raw exhaust of R case with $n_{\text{sa}} = 0.25$. The figure is scaled vertically with a factor of 10.

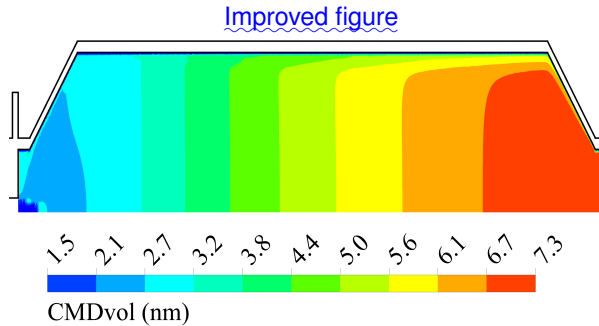


Figure 9. ~~Volatile~~The volatile nucleation mode CMD in the aging chamber region when there is $[\text{H}_2\text{SO}_4] = 1.47 \times 10^{11} \text{ cm}^{-3}$ in raw exhaust of R case with $n_{\text{sa}} = 0.25$. The figure is scaled vertically with a factor of 10.

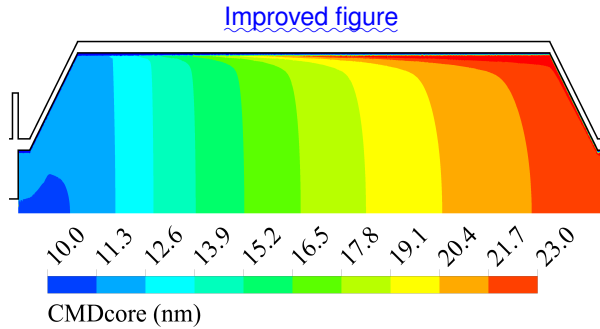


Figure 10. ~~Core~~ The core mode CMD in the aging chamber region when there is $[\text{H}_2\text{SO}_4] = 1.47 \times 10^{11} \text{ cm}^{-3}$ in raw exhaust of R case with $n_{\text{sa}} = 0.25$. The figure is scaled vertically with a factor of 10.

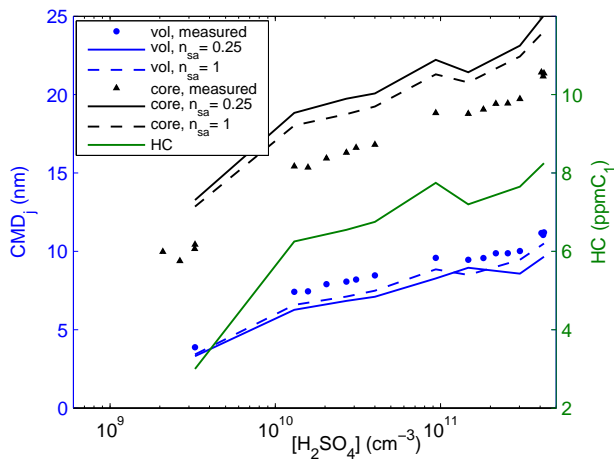


Figure 11. Measured and simulated CMD_{vol} and CMD_{core} and hydrocarbon vapor amount in raw exhaust as a function of raw exhaust sulfuric acid vapor concentration in R cases. Measurement data are obtained from Rönkkö et al. (2013).

Deleted figure
Path lines in PTD region for Lagrangian simulation.

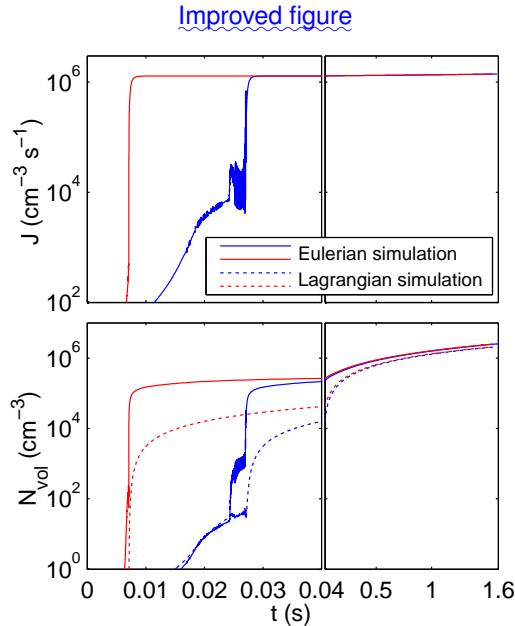


Figure 12. Nucleation rate and particle concentration as a function of time on three the path lines. Nucleation rate profiles are the same in both simulations. The right Note the different time scales; the left plots present show the ends very beginning of the paths curves as zoomed.

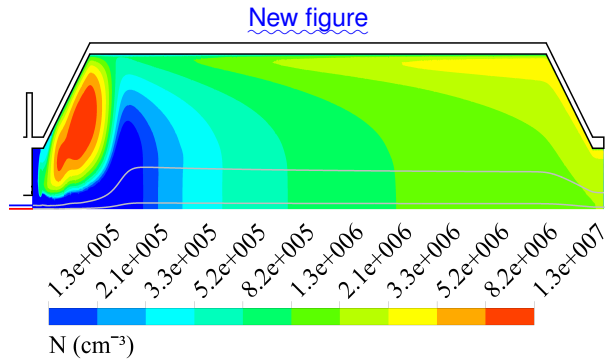


Figure 13. Particle concentration in the aging chamber region when there is $[\text{H}_2\text{SO}_4] = 4.6 \times 10^{10} \text{ cm}^{-3}$ in raw exhaust of A case with $n_{\text{sa}} = 1$ and when turbulent diffusion for particles is neglected. The path lines are also shown. The figure is scaled vertically with a factor of 10.

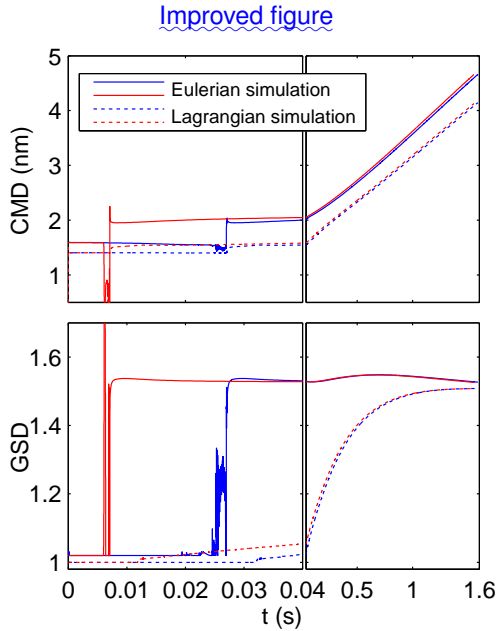


Figure 14. CMD_{vol} and GSD_{vol} as a function of time on three the path lines. The right plots present the ends of Note the paths different time scales.

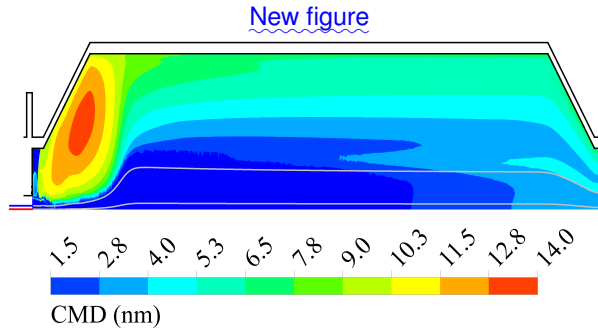


Figure 15. CMD in the aging chamber region when there is $[\text{H}_2\text{SO}_4] = 4.6 \times 10^{10} \text{ cm}^{-3}$ in raw exhaust of A case with $n_{\text{sg}} = 1$ and when turbulent diffusion for particles is neglected. The path lines are also shown. The figure is scaled vertically with a factor of 10.

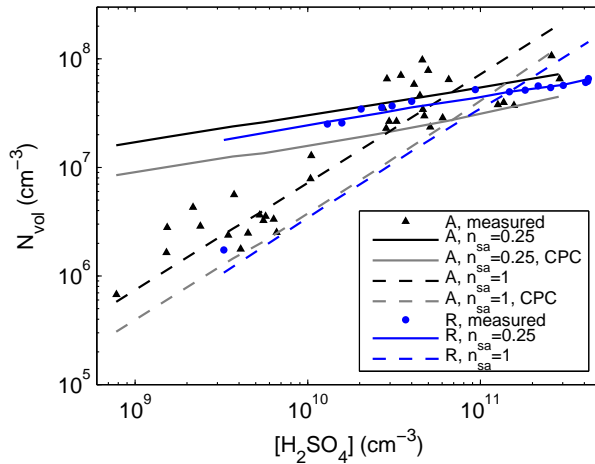


Figure 16. Measured and simulated volatile nucleation mode concentrations as a function of raw exhaust sulfuric acid vapor concentration. Particle concentrations are normalized to raw exhaust by dilution ratio 12. Measurement data for R cases are obtained from Rönkkö et al. (2013) and for A cases from Arnold et al. (2012).